NASA CR-134656
BAC Report No. 8654-953005

FINAL REPORT

NONDESTRUCTIVE TESTS OF REGENERATIVE CHAMBERS

By

G. A. MALONE
L. VECCHIES
R. WOOD

Prepared For

NATIONAL AERONAUTICS AND SPACE ADMINISTRATION

JUNE 1974

CONTRACT NAS 3-16800

Bell Aerospace Company DIVISION OF textron

POST OFFICE BOX ONE • BUFFALO, NEW YORK 14240

NOTICE

This report was prepared as an account of Government-sponsored work. Neither the United States, nor the National Aeronautics and Space Administration (NASA), nor any person acting on behalf of NASA:

A.) Makes any warranty or representation, expressed or implied, with respect to the accuracy, completeness, or usefulness of the information contained in this report, or that the use of any information, apparatus, method, or process disclosed in this report may not infringe privately-owned rights; or

B.) Assumes any liabilities with respect to the use of, or for damages resulting from the use of, any information, apparatus, method or process disclosed in this report.

As used above, "person acting on behalf of NASA" includes any employee or contractor of NASA, or employee of such contractor, to the extent that such employee or contractor of NASA or employee of such contractor prepares, disseminates, or provides access to any information pursuant to his employment or contract with NASA, or his employment with such contractor.

1. Report No.	2. Government Accession No.	3. Recipient's Catalog No.
NASA CR-134656		

4. Title and Subtitle	5. Report Date
Nondestructive Tests of Regenerative Chambers	June 1974
	6. Performing Organization Code

7. Author(s)	8. Performing Organization Report No.
G. A. Malone, L. Vecchies and R. Wood	BAC 8654-953005
	10. Work Unit No.

9. Performing Organization Name and Address	11. Contract or Grant No.
Bell Aerospace Company Division of Textron P.O. Box 1 Buffalo, New York 14240	NAS 3-16800
	13. Type of Report and Period Covered
12. Sponsoring Agency Name and Address	Contractor Report
National Aeronautics and Space Administration Washington, D.C. 20546	14. Sponsoring Agency Code

15. Supplementary Notes

Project Manager, Rudolph A Duscha, Chemical and Nuclear Rocket Procurement Section, NASA Lewis Research Center, Cleveland, Ohio

16. Abstract

The objective of this program was to define the capabilities and limitations of nondestructive evaluation methods to detect and locate bond deficiencies in regeneratively cooled thrust chambers for rocket engines. Nondestructive evaluation methods used were those of demonstrated capability from previous work under Contract NAS 3-14376 (NASA Report CR-120980).

Under this contract, flat test panels and a cylinder were produced to simulate regeneratively cooled thrust chamber walls. Planned defects with various bond integrities were produced in the panels to evaluate the sensitivity, accuracy, and limitations of nondestructive methods to define and locate bond anomalies. Holography, acoustic emission, and ultrasonic "C" scan were found to yield sufficient data to discern bond quality when used in combination and in selected sequences. Bonding techniques included electroforming and brazing. Materials of construction included electroformed nickel bonded to Nickel 200 and OFHC copper, electroformed copper bonded to OFHC copper, and 300 series stainless steel brazed to OFHC copper. Variations in outer wall strength, wall thickness, and defect size were evaluated for nondestructive test response.

17. Key Words (Suggested by Author(s))	18. Distribution Statement
Nondestructive Tests Regenerative Chambers Metal Bond Integrity	Unclassified - Unlimited This is the first volume of a two volume report. See Report No. NASA CR-134657 for the second volume.

19. Security Classif. (of this report)	20. Security Classif. (of this page)	21. No. of Pages	22. Price*
Unclassified	Unclassified	92	

* For sale by the National Technical Information Service, Springfield, Virginia 22151

NASA CR-134656
BAC Report No. 8654-953005

FINAL REPORT

NONDESTRUCTIVE TESTS OF REGENERATIVE CHAMBERS

by

G. A. Malone
L. Vecchies
R. Wood

Prepared for
National Aeronautics and Space Administration

June 1974

Technical Management
NASA, Lewis Research Center
Cleveland, Ohio

Chemical Propulsion Division

Rudolph A. Duscha

Bell Aerospace Company
P. O. Box 1
Buffalo, N. Y. 14240

FOREWORD

The work reported herein was performed for NASA-Lewis Research Center under Contract NAS 3-16800 titled "Nondestructive Tests for Regenerative Chambers". Mr. R. A. Duscha was the NASA Project Manager.

The authors wish to acknowledge important contributions to this report by several individuals. These include the treatment of braze bonding by F. M. Pruett and R. L. Brown, electroforming assistance by J. W. Chase, nondestructive evaluation assistance by R. Stauffis, and metallographic analysis by J. Salvaggi.

Mr. G. A. Malone, co-author of this report, was Program Manager. Messrs. L. Vecchies and R. Wood were responsible for the nondestructive evaluation work conducted.

ABSTRACT

The objective of this program was to define the capabilities and limitations of nondestructive evaluation methods to detect and locate bond deficiencies in regeneratively cooled thrust chambers for rocket engines. Nondestructive evaluation methods used were those of demonstrated capability from previous work under Contract NAS 3-14376 (NASA Report CR-120980).

Under this contract, flat test panels and a cylinder were produced to simulate regeneratively cooled thrust chamber walls. Planned defects with various bond integrities were produced in the panels to evaluate the sensitivity, accuracy, and limitations of nondestructive methods to define and locate bond anomalies. Holography, acoustic emission, and ultrasonic "C" scan were found to yield sufficient data to discern bond quality when used in combination and in selected sequences. Bonding techniques included electroforming and brazing. Materials of construction included electroformed nickel bonded to Nickel 200 and OFHC copper, electroformed copper bonded to OFHC copper, and 300 series stainless steel brazed to OFHC copper. Variations in outer wall strength, wall thickness, and defect size were evaluated for nondestructive test response.

CONTENTS

ILLUSTRATIONS

TABLES

I - SUMMARY

Flat test panels were designed for evaluation of the capability and limitations of nondestructive test methods to detect and locate bonds of various integrities. The panels contained manifolded passages to simulate actual regeneratively cooled thrust chamber wall structures. This configuration permitted pressurization during nondestructive evaluation. Specific bond integrities were assigned to each test panel and defects were limited to the center bonding rib. No more than one defect was planned for any panel.

Selection of acoustic emission, holography and ultrasonic "C" scan as the nondestructive methods to be used in this program was based on favorable experience with these techniques in previous work, Contract NAS 3-14376.

The material combinations bonded to produce panels for this investigation included electroformed nickel on Nickel 200, electroformed nickel on OFHC Copper, electroformed copper on OFHC Copper and 300 Series Stainless Steel brazed to OFHC Copper. In addition, a test cylinder with internal passages was produced. from OFHC Copper and bonded by electroforming an outer close-out shell of nickel.

Initial panels were tested to confirm bond strength and establish characteristic performance of acoustic emission equipment for various bond integrities. Special standard panels were fabricated to calibrate and characterize each nondestructive evaluation method.

Where different techniques for utilizing an individual nondestructive test method were available, investigations were made to determine the best application for panel designs in this program.

Panels of the applicable material combinations were produced to contain various bond integrities, different coverplate thicknesses, variations in planned defect size, changes in coverplate mechanical properties, and varied coverplate surface flatness. Nondestructive test personnel were provided no knowledge of the planned bond integrities. All panels were nondestructively evaluated to determine bond quality and defect location. These panels were then destructively tested, bond strengths calculated, and metallurgical sections prepared for correlation of destructive test results with those of the nondestructive evaluation.

The test cylinder was nondestructively evaluated but not destructively tested.

Correlation of test data indicated that application of the three nondestructive test methods to evaluating bonds on these materials and structural configurations will provide a useful and accurate assessment of bond integrity. Additional definition of equipment response to certain structural variables to be expected in actual thrust chambers is still required. However, the results of this program indicate nondestructive evaluation will become an accepted means of thrust chamber surveillance testing.

II - INTRODUCTION

A conventional regeneratively cooled rocket thrust chamber is usually constructed by bonding a liner (inner wall) to a shell (outer wall) by means of electroforming the shell over the liner, brazing, or diffusion bonding. Coolant passages are usually produced in the liner by machining prior to the bonding of the outer shell.

Fabrication of such devices is critical from a standpoint that detection and location of inferior bonds or leakage paths for the coolant must be made as early as possible in the fabrication process. Otherwise, expensive and time consuming manifold joining, flow, proof, and hot fire testing will be uneconomically expended on a possibly defective piece of hardware.

Nondestructive evaluation appears to be the most desirable means of detecting bonding defects at an early stage. Preliminary work under Contract NAS 3-14376 was reported in Report NASA CR-120980 which indicated that ultrasonic "C" scan, holography and acoustic emission were nondestructive tests feasible for detecting inferior bonds in hollow-wall structures. This work was confined to a limited combination of construction material, mostly nickel and nickel alloys. The initial panel design employed and multiplicity of defects in the same panel provided data interpretation problems from a quantitative aspect.

The present work was a continuation of the development of nondestructive methods for evaluating regeneratively cooled

thrust chambers. Efforts were directed to further defining the quantitative response of individual bond defects to nondestructive examination. Additional construction materials were to be evaluated.

III. TASK I - DESIGN OF TEST PANELS AND CYLINDER

Test Panels fabricated in the previous work under Contract NAS3-14376 contained eight bonded ribs (lands) and nine coolant passages. Baseplates were produced from 3.175 mm. (0.125 inch) thick nickel 200 plates. Planned defects were produced on all bonding ribs, except in the case of full bonds. Although this design was satisfactory for demonstrating the feasibility of detecting bond defects by nondestructive means, the resulting data could not be used for quantitative determination of nondestructive test response to individual flaws by size or geometry.

The panel design in Contract NAS3-14376 required a baseplate of a thickness which frequently buckled simultaneously with the coverplate. Actual regeneratively cooled thrust chambers do not generally fail with buckling of both outer shell and inner liner. For this reason an improved panel design was required to more closely simulate production thrust chamber walls.

A. DESIGN OF FLAT TEST PANELS

The test panel design shown in Figure 1 was selected for use in this project. This panel contains three bonding ribs and four coolant channels with manifolds at each end for simultaneous pressurization. Since no more than one bond defect was planned on any single panel, the use of three bonding ribs was considered sufficient to provide reliable nondestructive test response. All defects were intentionally located on the center rib (second land).

By providing manifolds and pressurization ports at each end of the panel; it was possible to allow passage of fluids through the panel, to purge air from the passages during hydrostatic pressurization, and afford a means of removing channel filler materials necessary in the electroform method of bonding. The pressure fitting ports were placed in opposite corners of the panel to provide maximum freedom for positioning transducers for the acoustic emission equipment flaw locator system.

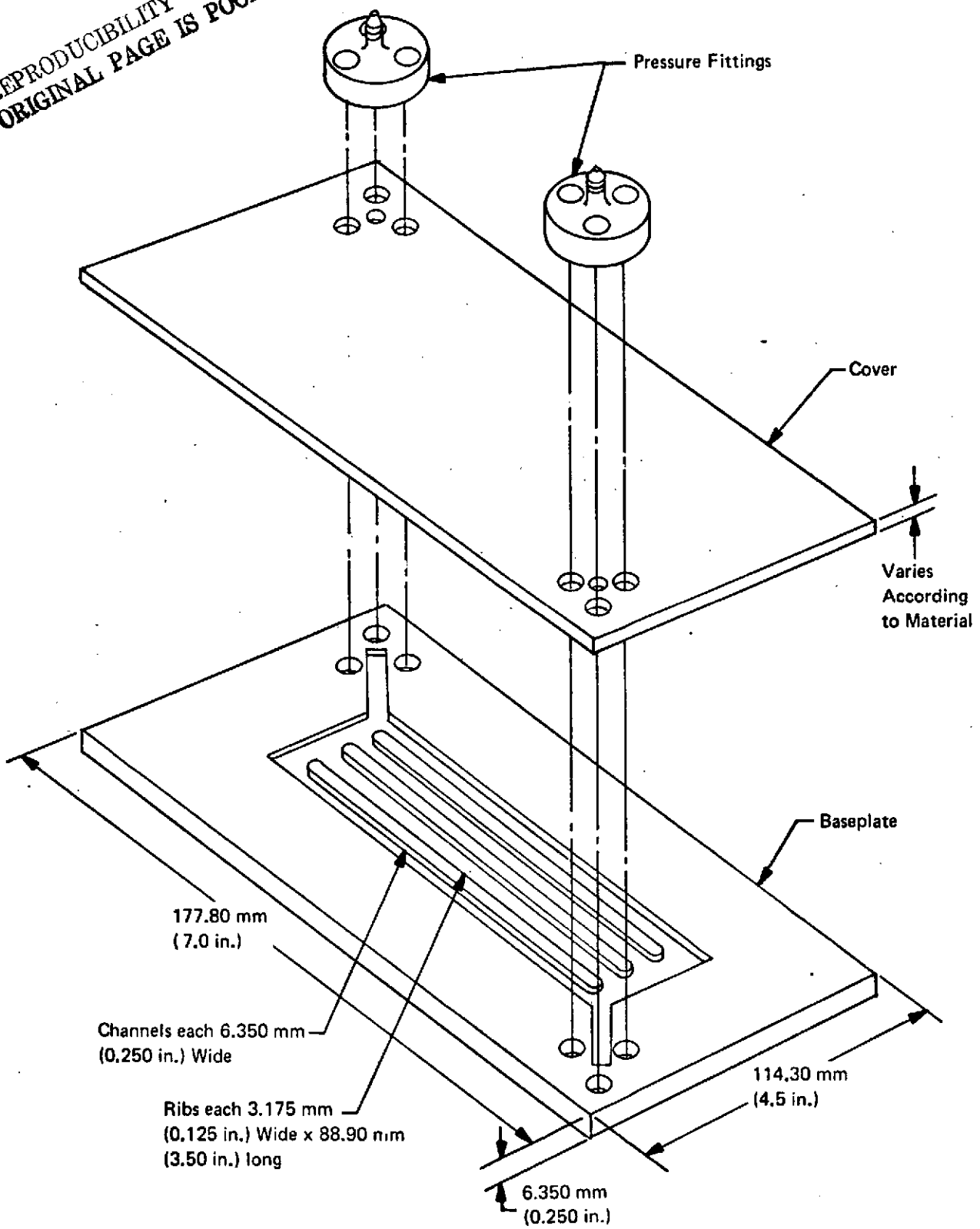

Figure 1. Panel Assembly Design - Flat Panels

It was desired that all panels be capable of destructive failure at 6.90×10^7 N/m.^{2} (10,000 psi) or less - the limiting capacity of the hydraulic pump used to pressurize during acoustic emission nondestructive evaluation. This would enable continued acoustic monitoring during the final destructive test required on each panel. Failure during destructive test was defined as evidence of external leakage or permanent deformation of the panel through bond failure or yielding of the weakest portion of either the coverplate or the base plate. The thicknesses employed in the baseplates and coverplates were critical and required knowledge of mechanical properties of the panel materials in order to determine desired thicknesses in the panel design.

To determine the channel dimensions necessary to respond to nondestructive evaluation (NDE) techniques at internal pressures to 6.90×10^7 N/m.^{2} (10,000 psi), formulas for buckling of a flexible loaded beam were applied as illustrated in Figure 2. For the initial tests to verify bond strengths for full, weak and non-bonds, the position for load concentration was assumed to be at the midpoint of each land in Figure 2. Bond strength verification test proved this assumption incorrect in that electroformed cover plates were too thick to fail at 6.90×10^7 N/m.^{2} (10,000 psi). Correction of stress concentration regions to the true channel width (dimension "L" in Figure 2) resulted in coverplate thicknesses which normally failed at the desired pressure limit.

The final thicknesses calculated for coverplates and baseplates are discussed under that portion of Section IV dealing with mechanical properties of materials used in this project.

Several panels were fabricated with variations to the rib-channel pattern shown in Figure 1. The basic differences in these panels were the width of the ribs and channels. These special

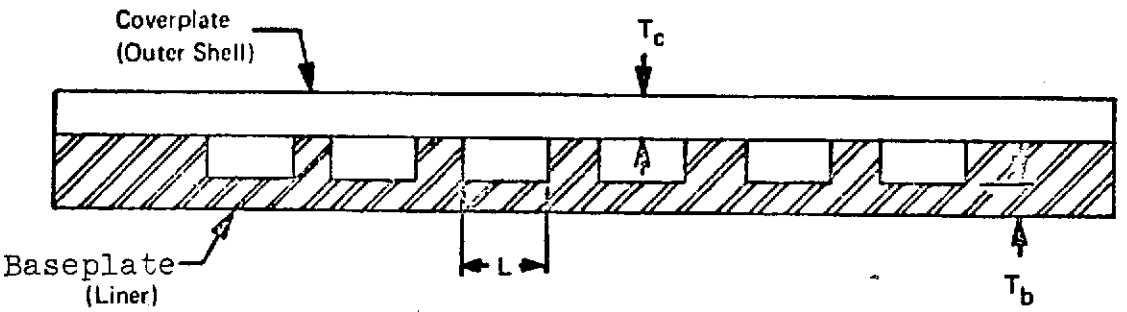

Approach to Panel Design:

The coverplate is considered to be a flexible loaded beam, segments of which are supported by the bonds at the lands or ribs. From Formulas for Stress and Strain, Raymond J. Roark, McGraw-Hill Publishing Company, 1965, the formulas which approximate this load situation, for buckling, are:

$$S = \frac{6M}{T^2}$$

$$M = \frac{P L^2}{24}$$

Where: S = Yield strength of material (psi)

L = Channel Width (inches)

P = Applied loading pressure (psig)

T = Structural member thickness (inches)

c = Subscript designating coverplate

b = Subscript designating baseplate

M = Moment (inch-pounds)

From these formulas, the required thicknesses can be determined for prevention of buckling failure at pressures necessary to fail the bond region. With buckling restrained, the failure loading on a single rib is directly related to the pressure loading on the two adjacent channels (excluding rib end effects).

Figure 2. Flat Panel Design Approach for Bond Testing

panels contained bonded ribs which were 1.5748 mm. (0.062 inch) wide and channels which were 3.1750 mm. (0.125 inch) wide. The purpose of these panels was to compare the effect of rib width on NDE response.

B. FLAT TEST PANEL REQUIREMENTS AND PLANNED BOND DEFECT PATTERNS

Table I lists the various types of panels to be fabricated for bond strength verification tests. Three types of bonds were required - non-bond, weak bond and full bond. All planned flaws were 25.4 mm (1.0 inch) long and located in the middle land. Two kinds of baseplate materials, Nickel 200 and OFHC copper, were used. The Nickel 200 baseplates were bonded to electroformed nickel coverplates. The OFHC copper baseplates were bonded to coverplates composed of electroformed nickel, electroformed copper and brazed 300 series stainless steel. The planned bond defects, where such were required, are illustrated for each test panel in Appendix Section A.

To properly calibrate and interpret nondestructive evaluation results, a set of standard test panels were prepared for each method of NDE - ultrasonic "C" scan, holography and acoustic emission. All panels in this group contained Nickel 200 baseplates and electroformed nickel coverplates. The flaw designs for these panels were not necessarily typical of those used in the remaining panels. These defects were applied for the purpose of determining NDE equipment response to flaw area, flaw size, coverplate thickness, and bond strength. Table II lists the panels required as standards. The flaw patterns for these panels are shown for each test specimen in Appendix Section B. These panels were not subject to destructive test.

Table III lists the test panels required in the NDE equipment limitations investigation. These panels were fabricated to contain planned bond defects of various sizes, coverplate

TABLE I - BOND STRENGTH VERIFICATION PANELS

MATERIAL COMBINATIONS		NUMBER OF PANELS REQUIRED		
BASEPLATE	COVERPLATE	FULL BOND	WEAK BOND	NONBOND
Nickel 200	EF Nickel	1	2	1
OFHC Copper	EF Nickel	1	2	1
OFHC Copper	EF Copper	1	2	1
OFHC Copper	Brazed 300 Series Stainless Steel	1	2	1

TABLE II - NDE STANDARD PANELS FOR EQUIPMENT CALIBRATION

(ALL PANELS HAVE NICKEL 200 BASEPLATES AND ELECTROFORMED NICKEL COVERPLATES)

	NUMBER OF PANELS REQUIRED		
PANEL APPLICATION	FULL BOND	WEAK BOND	NONBOND
Ultrasonic "C" Scan:			
Thickness Sensitivity	0	0	3
Pressure Response	0	0	1
Holography:			
Stress Method	0	0	2
Bond Strength	1	2	0
Flaw Size	0	0	2
Acoustic Emission:			
Bond Strength Study	1	2	0
Nonbond Study	0	0	2
Flaw Location	0	1	0

TABLE III - NDE TEST PANELS FOR EQUIPMENT LIMITATION INVESTIGATION

MATERIAL COMBINATION			NUMBER OF PANELS REQUIRED		
BASEPLATE	COVERPLATE	SUBJECT OF INVESTIGATION	FULL BOND	WEAK BOND	NONBOND
Nickel 200	EF Nickel	Standard Flaw Area	1	2	1
		Second Flaw Area	0	2	1
		Coverplate Thickness	1	2	1
		Coverplate Strength	1	2	1
		Surface Flatness	1	1	1
OFHC Copper	EF Nickel	Standard Flaw Area	1	2	1
		Second Flaw Area	0	2	1
		Coverplate Thickness	1	2	1
		Coverplate Strength	1	2	1
OFHC Copper	EF Copper	Standard Flaw Area	1	2	1
		Second Flaw Area	0	2	1
		Coverplate Thickness	1	2	1
		Coverplate Strength	1	2	1
OFHC Copper	Brazed 300 Series Stainless Steel	Standard Flaw Area	1	2	1
		Second Flaw Area	0	2	1
		Coverplate Thickness	1	2	1

thicknesses, coverplate strengths, and coverplate surface flatnesses. The material combinations discussed for bond strength verification panels were used. The flaw patterns for each of these panels are shown in Appendix Section C.

C. CYLINDER DESIGN AND FLAW PATTERN

To evaluate the response limitations of NDE equipment on curved surfaces, a test cylinder was designed for study. Figure 3 illustrates the cylinder construction. The liner was required to be OFHC copper and the outer shell was electroformed nickel. Three commonly manifolded test sections were provided in the liner. Each section contained a different bond type - full, weak and nonbond. Four bonding ribs and five channels were provided in each test section. Pressure fittings were applied to the internal diameter surface to minimize obstruction to the outer shell where flaw locator transducers would be used. Figure 4 shows a planar map of the bonding surface and location of planned flaws.

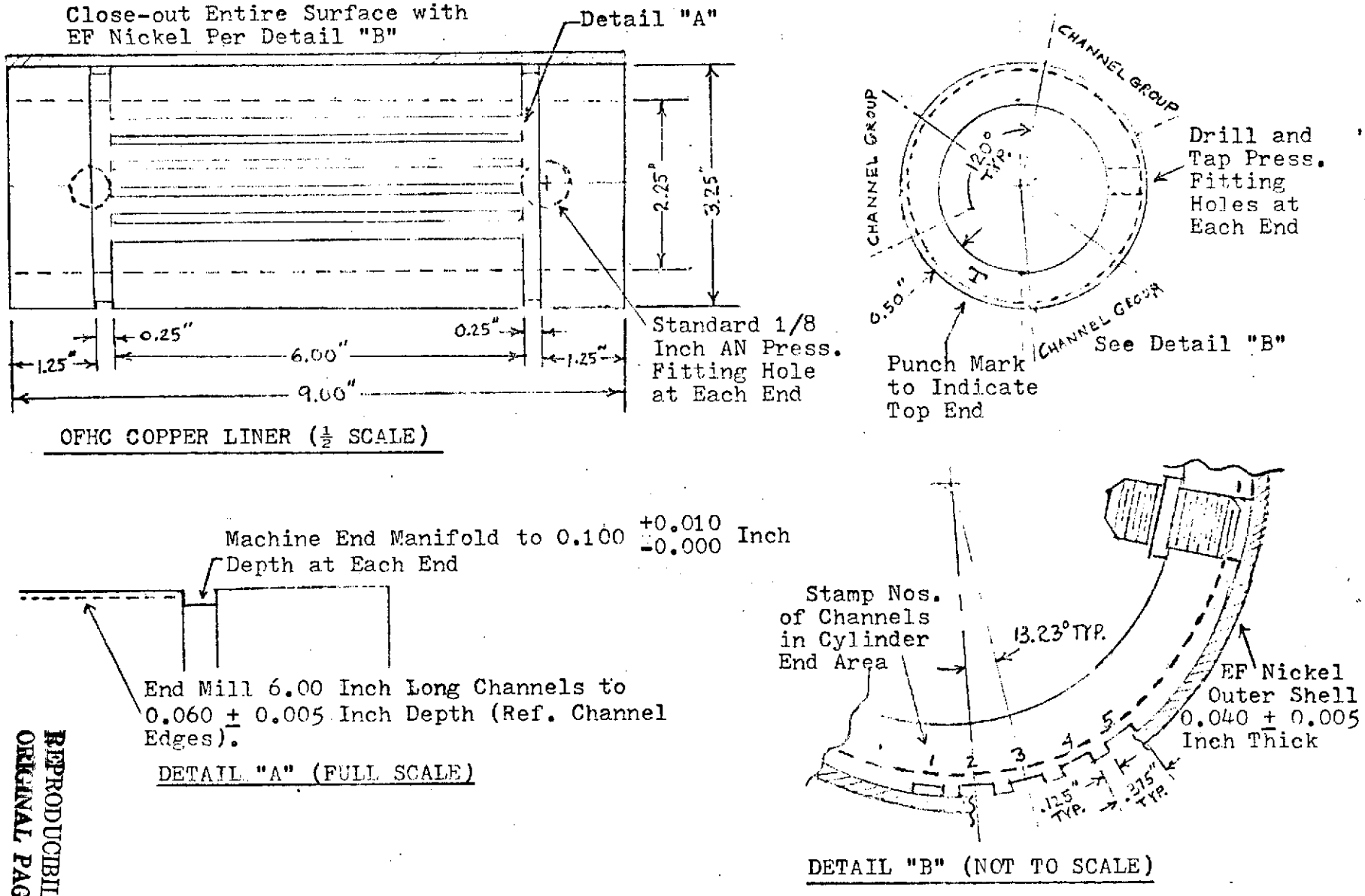

Figure 3 - Test Cylinder Design

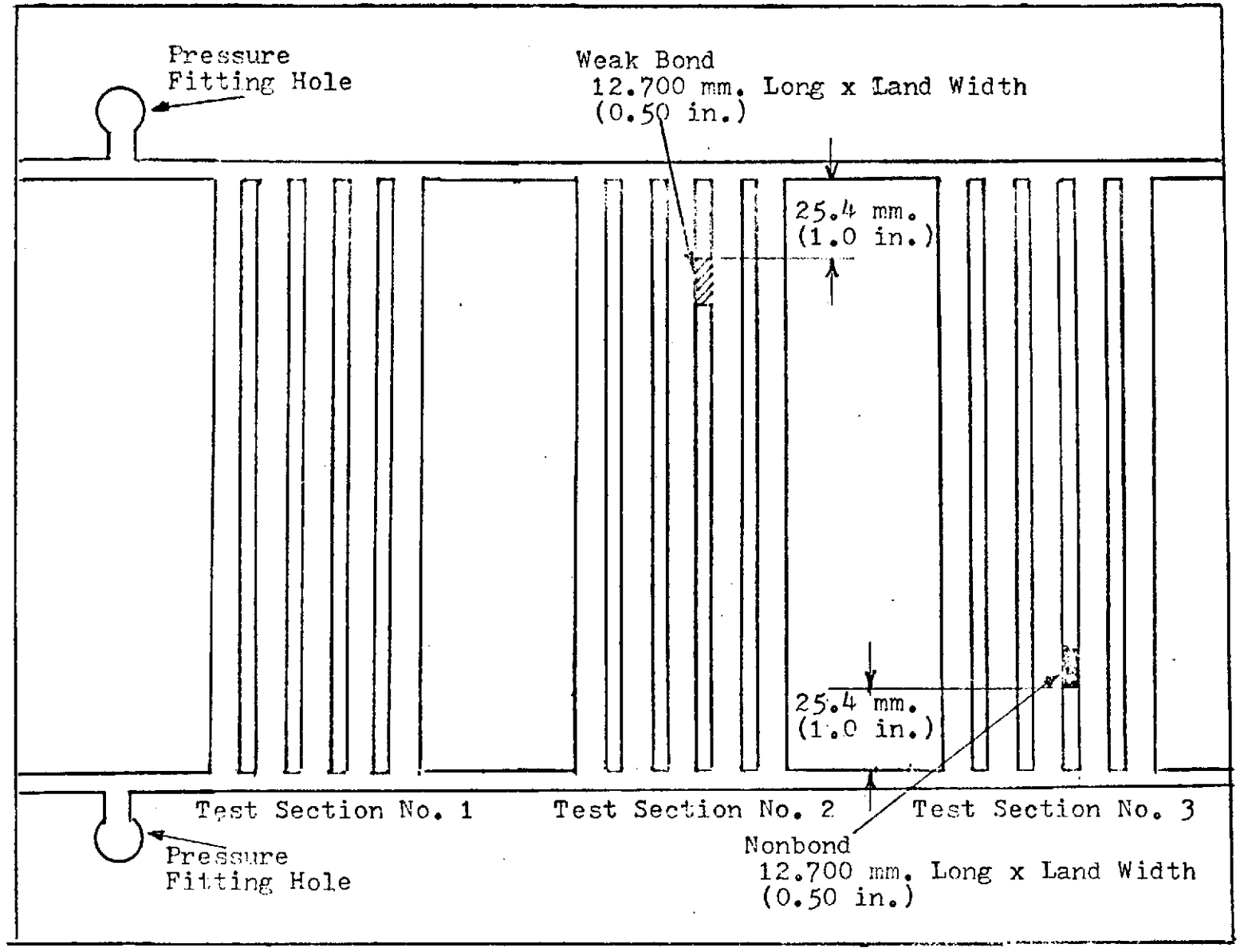

Figure 4 - Cylinder Planned Flaw Pattern

IV. TASK II - BOND STRENGTH VERIFICATION AND PANEL FABRICATION

It was necessary to finalize the panel design and assure that procedures for producing full, weak and nonbonds were reliable, prior to fabricating the panels required to calibrate the NDE test equipment and investigate the equipment limitations. Processes for producing bonds of various strengths had been developed for electroformed nickel coverplates on Nickel 200 baseplates in previous work reported under Contract NAS3-14376. Processes for similar bonds were now required for electroformed nickel and copper on OFHC Copper and for stainless steel brazed to OFHC Copper.

Coverplate thickness required definition based on actual mechanical properties of the construction materials to finalize the panel design. Some panels used in the investigation of NDE equipment limitations would require a change in mechanical strength of the electroformed coverplate and it was necessary to demonstrate that this could be achieved in both nickel and copper.

Most test panels were fabricated as planned and successfully utilized in the program. A few panels contained unplanned defects which were not apparent until they were nondestructively evaluated and subsequently metallurgically analyzed.

A. PANEL FABRICATION MATERIALS

1. OFHC Copper Baseplates

0.635 mm (0.25 inch) thick OFHC Copper plate, conforming to the requirements of Specification ASTM B-152, was used in the fabrication of panels requiring copper as the baseplate material. Mechanical property tests were performed on the material and test results and certified chemical analysis are shown in Table IV. Samples of the OFHC Copper were subjected to the thermal cycle to be used in brazing with stainless steel coverplates and also tested for mechanical properties.

TABLE IV - MECHANICAL AND CHEMICAL PROPERTIES OF OFHC COPPER BASEPLATES

Condition: Cold Rolled, Light Anneal

PROPERTY	AS RECEIVED		THERMALLY TREATED PER BRAZING CYCLE	
	$MN/m.^2$	Kpsi	$MN/m.^2$	Kpsi
Ultimate Strength	244.3	35.4	212.5	30.8
Yield Strength	193.2	28.0	52.4	7.6
Elongation in 50.8 mm.	47	-	59	-
(2.0 in)	-	47	-	59
Chemical Analysis:	Copper	Oxygen		
Required	99.95 min.	0.000		
Actual	99.99	0.000		

2. Nickel 200 Baseplates

0.635 mm. (0.25 inch) thick Nickel 200 plate was used in the manufacture of all test panels requiring nickel baseplates. This material was in the cold rolled/annealed condition conforming to Specification ASTM B-162. The certified mechanical properties and chemical analysis of this material are shown in Table V.

TABLE V - MECHANICAL AND CHEMICAL PROPERTIES OF NICKEL 200 BASEPLATES

Heat No. N1997A

Condition: Cold Rolled, Annealed

	$MN/m.^2$	Kpsi
Ultimate Strength	420.9	61.0
Yield Strength	213.9	31.0
Elongation in 50.8 mm. (2.0 in.) %	48	48

Chemical Analysis %

	C	Mn	Fe	S	Si	Cu	Ni
Required:	0.15 Max.	0.35 Max.	0.40 Max.	0.01 Max.	0.35 Max.	0.25 Max.	99.0 Min.
Actual:	0.03	0.26	0.03	0.005	0.03	0.01	99.61

3. Electroformed Nickel Coverplates

All electroformed nickel was produced from nickel sulfamate electrolyte. Electroformed nickel of two different mechanical strengths was required to demonstrate the effect of this variable on NDE results. The variation of mechanical properties was achieved by changing the current density (rate of electrodeposition). The higher strength nickel was used throughout the investigation since the mechanical properties were similar to those employed in regeneratively cooled chamber electroforming. The lower strength nickel was used to make coverplates on four special test panels in the equipment limitations study(Task IV).

Sulfur depolarized nickel anodes in titanium anode baskets were used in order to operate the electrolyte at low chloride levels and minimize residual stress in the deposits. Continuous carbon treatment was employed to remove organic contamination which might affect mechanical properties. Solution agitation was accomplished by chemical pumps and filter pumps.

Special test cylinders were electroformed and sectioned into tensile test strips to verify mechanical properties of the deposited nickel. These strips were milled to standard ASTM requirements for testing. The electrolyte composition, operating parameters, and electrodeposit mechanical properties are shown in Table VI.

4. Electroformed Copper Coverplates

All electroformed copper was produced from a bright acid copper electrolyte. Electroformed copper of two different mechanical strengths was required to demonstrate the effect of this variable on NDE results. This variation was produced by variation of the current density for electrodeposition. The higher strength copper was used throughout the investigation, except

TABLE VI - ELECTROFORMED NICKEL MECHANICAL PROPERTIES AND ELECTROLYTE DATA

	HIGH STRENGTH		LOW STRENGTH	
Mechanical Properties:	$MN/m.^2$	kpsi	$MN/m.^2$	kpsi
Ultimate Strength	697	101	524	76
Yield Strength	462	67	331	48
Elongation, % in 50.8 mm. (2 in.)	9		12	
Electrolyte Analysis:	g/l	oz./gal.	g/l	oz./gal.
Nickel Metal	74.2	9.9	74.2	9.9
Nickel Chloride	3.07	0.41	3.07	0.41
Boric Acid	33.0	4.4	33.0	4.4
Wetting Agent	None		None	
pH	4.2		4.2	
Temperature	°K	°F	°K	°F
	314	105	316	110
Current Density	$Amp/m.^2$	$Amp/Ft.^2$	$Amp/m.^2$	$Amp/Ft.^2$
	279	30	651	70

TABLE VII - ELECTROFORMED COPPER MECHANICAL PROPERTIES AND ELECTROLYTE DATA

	HIGH STRENGTH		LOW STRENGTH	
Mechanical Properties:	$MN/m.^2$	kpsi	$MN/m.^2$	kpsi
Ultimate Strength	421	61	324	47
Yield Strength	338	49	262	38
Elongation, % in 50.8 mm. (2 in.)	12		27	
Electrolyte Analysis:	g/l	oz./gal.	g/l	oz./gal.
Copper Sulfate	239.7	32	239.7	32
Sulfuric Acid	74.9	10	74.9	10
Brightener	0.4% by vol.		0.4% by vol.	
Leveler	0.1% by vol.		0.1% by vol.	
Temperature	°K	°F	°K	°F
	305	90	305	90
Current Density	$Amp/m.^2$	$Amp/Ft.^2$	$Amp/m.^2$	$Amp/Ft.^2$
	465	50	929	100

for those panels used in the coverplate strength portion of the equipment limitations investigation. For these four panels the low strength copper was used to electroform coverplates. Mechanical properties and electrolyte operating parameters are shown in Table VII.

Phosphorous bearing OFHC copper anodes were used in the electroforming solution to minimize anode passivity over a wide range of current density. Continuous filtration was employed to maintain good deposit quality. Commerical levelling and brightening agents were used in concentrations known to produce desired surface quality and controlled mechanical properties. Periodic carbon treatment was used to remove by-products of additive degradation. New levelling and brightening agents were added on these occasions.

Cathode agitation was employed to maintain adequate solution circulation at the surface being electroformed. Plastic frame shields were mounted on the face of the baseplates to minimize edge build-up and excess edge nodule (dendrite) growth. Figure 5 illustrates the copper electroforming facility.

5. Brazed Stainless Steel Coverplates

300 Series Stainless Steel was required as coverplate material for the braze fabrication of test panels. Two thicknesses of material were necessary to evaluate NDE response to coverplate stressing. Both materials were procured to appropriate military specifications as shown in Table VIII. For the thin coverplates (1.2 mm. or 0.048 inch thickness), Type 304L was selected. For the four panels requiring a different thickness, Type 347 (2.337 mm. or 0.092 inch thickness) was used for coverplates. Table VIII represents mechanical property data and nominal (certified) analyses on each alloy. Included in this table are mechanical properties of each alloy after exposure to the braze cycle temperature.

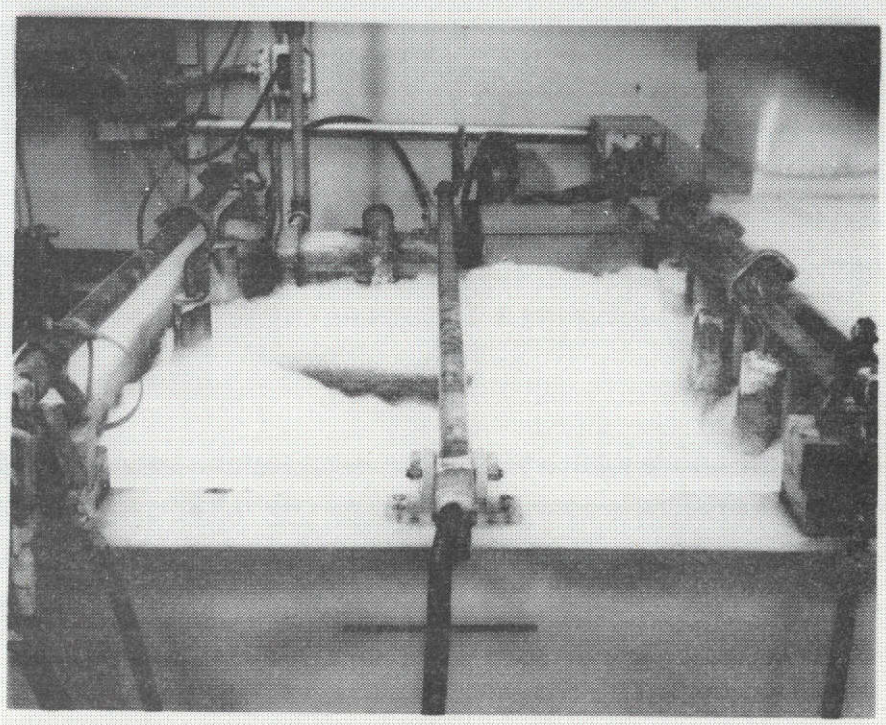

Figure 5. Acid Copper Electroforming Facility

TABLE VIII - STAINLESS STEEL MECHANICAL PROPERTIES AND CHEMICAL ANALYSIS

	STAINLESS STEEL, TYPE 304L				STAINLESS STEEL, TYPE 347			
	As Received		Braze Cycled		As Received		Braze Cycled	
Nominal Thickness	mm.	in.	mm.	in.	mm.	in.	mm.	in.
	1.219	0.048	1.219	0.048	2.337	0.092	2.337	0.092
Mechanical Properties	MN/m^2	Kpsi	MN/m^2	Kpsi	MN/m^2	Kpsi	MN/m^2	Kpsi
Ultimate Strength	612.0	88.7	588.6	85.3	661.7	95.9	636.9	92.3
Yield Strength	286.4	41.5	259.4	37.6	338.8	49.1	309.8	44.9
Elongation, % in 50.8 mm. (2.0 in.)	52		53		43		42	
Chemical Analysis Certified to Meet: (Values in %)	Specification MIL-S-4043B				Specification MIL-S-6721B			
	Carbon	0.03 Max.			Carbon	0.08 Max.		
	Manganese	2.00 Max.			Manganese	2.00 Max.		
	Phosphorus	0.040 Max.			Phosphorus	0.040 Max.		
	Sulfur	0.030 Max.			Sulfur	0.030 Max.		
	Chromium	18.00 - 20.00			Chromium	17.00 - 19.00		
	Nickel	8.00 - 11.00			Nickel	9.00 - 13.00		
	Silicon	1.00 Max.			Silicon	0.50 - 1.00		
	Molybdenum	0.50 Max.			Molybdenum	1.50 Max.		
	Copper	0.50 Max.			Copper	0.50 Max.		
	Iron	Remainder			Columbium + Tantalum	10 x Carbon to 1.25 Max.		
					Iron	Remainder		

6. Braze Alloy

The braze alloy used was AWS-ASTM Classification BAg-18. This alloy composition is sixty percent silver, thirty percent copper, and ten percent tin. The tin content promotes wetting of the stainless steel. The brazing range for the alloy is 991.5 to 1116.5°K (1325 to 1550°F).

B. DETERMINATION OF PANEL PLATE THICKNESS REQUIREMENTS

Theoretical baseplate and coverplate thicknesses were determined from the formulas in Figure 2. It was expected that the full bond panels would be the most difficult to destruct at, or below, a pressure of 69 $MN/m.^2$ (10,000 psi). From Figure 2, the thickness was calculated as:

$$T^2 = \frac{6M}{S} = \frac{6\ PL^2}{24\ S}$$

where: P = 69 $MN/m.^2$ (10,000 psi)

L = 9.525 mm. (0.375 in.), assuming the load concentration as occurring at the mid-point of the width of each land.

S = Yield strength of structural plate.

T = Thickness

For the mechanical properties previously shown, the non-buckling thicknesses were calculated as shown in Table IX.

TABLE IX

CALCULATED COVERPLATE AND BASEPLATE NONBUCKLING THICKNESSES

Baseplates	mm.	inches
OFHC Copper, As Received	2.845	0.112
OFHC Copper, Braze Cycled	5.461	0.215
Nickel 200	2.692	0.106
Coverplates		
EF Nickel (High Strength)	1.829	0.072
EF Copper (High Strength)	2.159	0.085
Stainless Steel, Type 304L	2.464	0.097
Stainless Steel, Type 347	2.235	0.088

It was desired that the baseplates not bulge or buckle during pressurized nondestructive evaluation or in destructive test. Use of 6.350 mm. (0.25 inch) thick baseplates provided the necessary thickness in accordance with Table IX calculations. Calculated thicknesses were found to be excessive as demonstrated in bond strength verification panel destructive tests. Electroformed copper and nickel full bond panels would not fail at 69 $MN/mm.^2$ (10,000 psi). Also, electroformed nickel weak bond panels failed at unexpectedly high pressures.

The coverplate thicknesses were recalculated using the experience obtained with the bond strength verification panels. Weak bond panels were considered the critical panels and assigned a desired coverplate failure and buckling pressure of 3.45 $MN/m.^2$ (5,000 psi). Also, the dimension "L" in the buckling formula was changed to represent the actual channel width. The new coverplate thickness calculations are shown in Table X.

TABLE X - COVERPLATE THICKNESS CALCULATIONS FOR WEAK BOND FAILURE WITH BUCKLING AT 34.5 $MN/m.^2$ (5,000 psi)

	mm.	inches
Electroformed Nickel (High Strength)	0.864	0.034
Electroformed Nickel (Low Strength)	1.016	0.040
Electroformed Copper (High Strength)	1.016	0.040
Electroformed Copper (Low Strength)	1.143	0.045
Stainless Steel, Type 304L	1.168	0.046
Stainless Steel, Type 347	1.067	0.042

The above coverplate thicknesses were approximately those used for test panels in the equipment limitations investigation (Task IV). These thicknesses provided planned bond failures at desired test pressures. The electroformed copper thicknesses were increased to about 1.270 mm. (0.050 in.) based on actual results in the bond strength verification tests. Type 304L stainless steel was selected due to material availability at the desired thickness. Type 347 stainless steel was used as coverplates where a different thickness was required.

The thickness of coverplates used on standard panels for NDE equipment calibration were not necessarily those in Table X. Thicknesses were often thinner or thicker to evaluate equipment response over a wide range of coverplate conditions.

C. FABRICATION OF TEST PANELS

1. Fabrication of Baseplates

Baseplates for all electroformed test panels and standards used in this project were electric discharge machined to produce the channel and manifold pattern. Electrodes for producing the channel pattern in Nickel 200 baseplates were made from graphite. The electrodes for fabricating the passages in copper were made from a copper-graphite composition material for improved electrode wear. Figure 6 illustrates an electrode machined from the composition material. Figure 7 shows a graphite electrode mounted in the electric discharge machining fixture. This electrode was used to produce the 1.524 mm (0.060 inch) wide land pattern.

Electric discharge machining of OFHC copper was found to be slow - even with the special electrode material. To accelerate baseplate fabrication, the OFHC copper for brazed panels was milled on a high speed template tracing machine. Figure 8 shows a milled copper baseplate (at the left) and an electric discharge machined plate (at the right). Figure 9 represents a typical electric discharge machined Nickel 200 baseplate with 3.175 mm (0.125 inch) wide lands and 6.350 mm (0.25 inch) wide channels.

All baseplates were stamped with test panel identification numbers after machining. The plates were then solvent degreased, alkaline cleaned and briefly treated in a solution of nitric acid containing ferric chloride to etch away the recast metal from the electric discharge machining or cold work from the milling.

Figure 6. Copper-Graphite Composition Electrode for Electric Discharge Machining Copper Baseplates

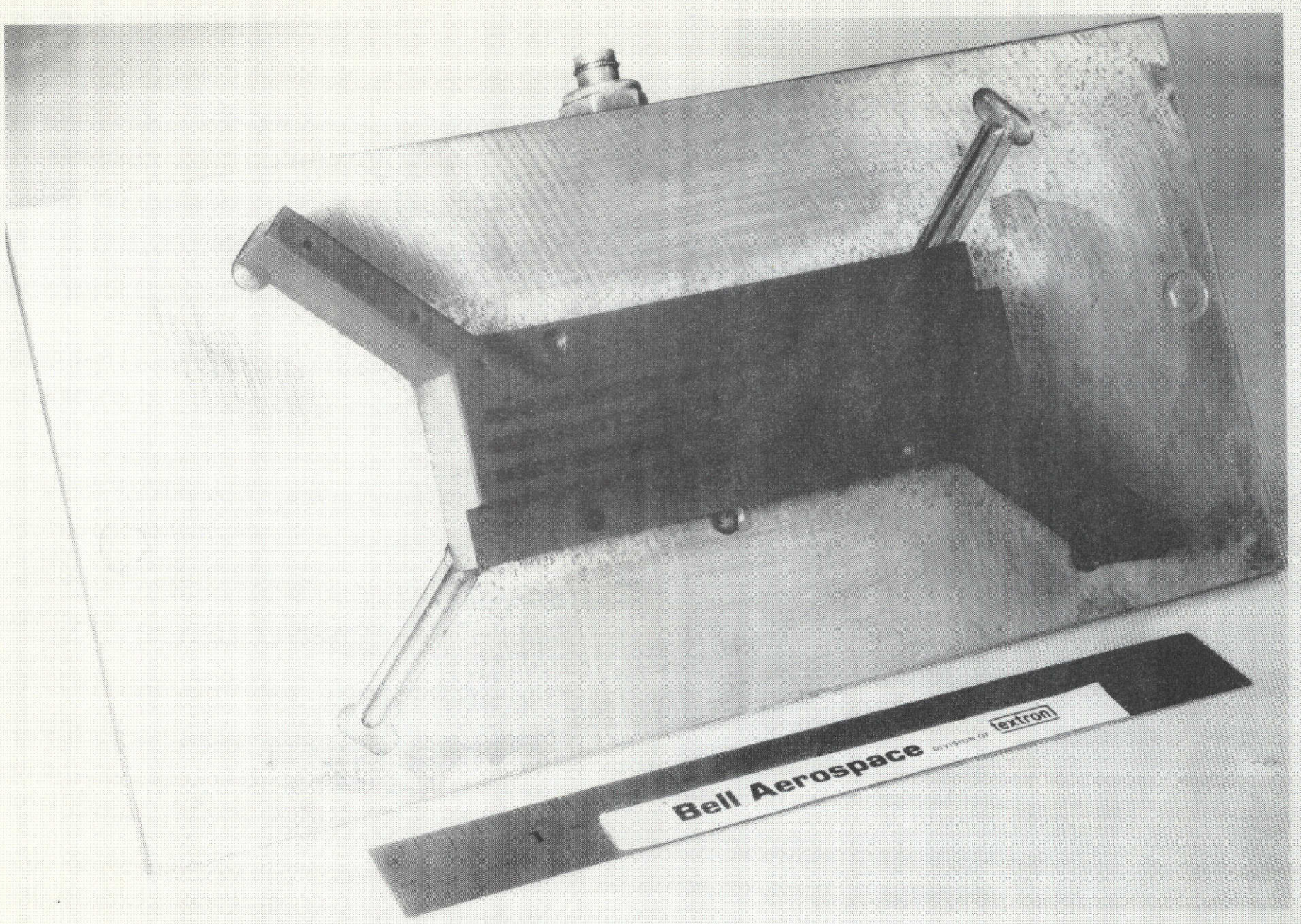

Figure 7. Graphite Electrode and Holding Fixture for Electric Discharge Machining of Nickel 200 Baseplates

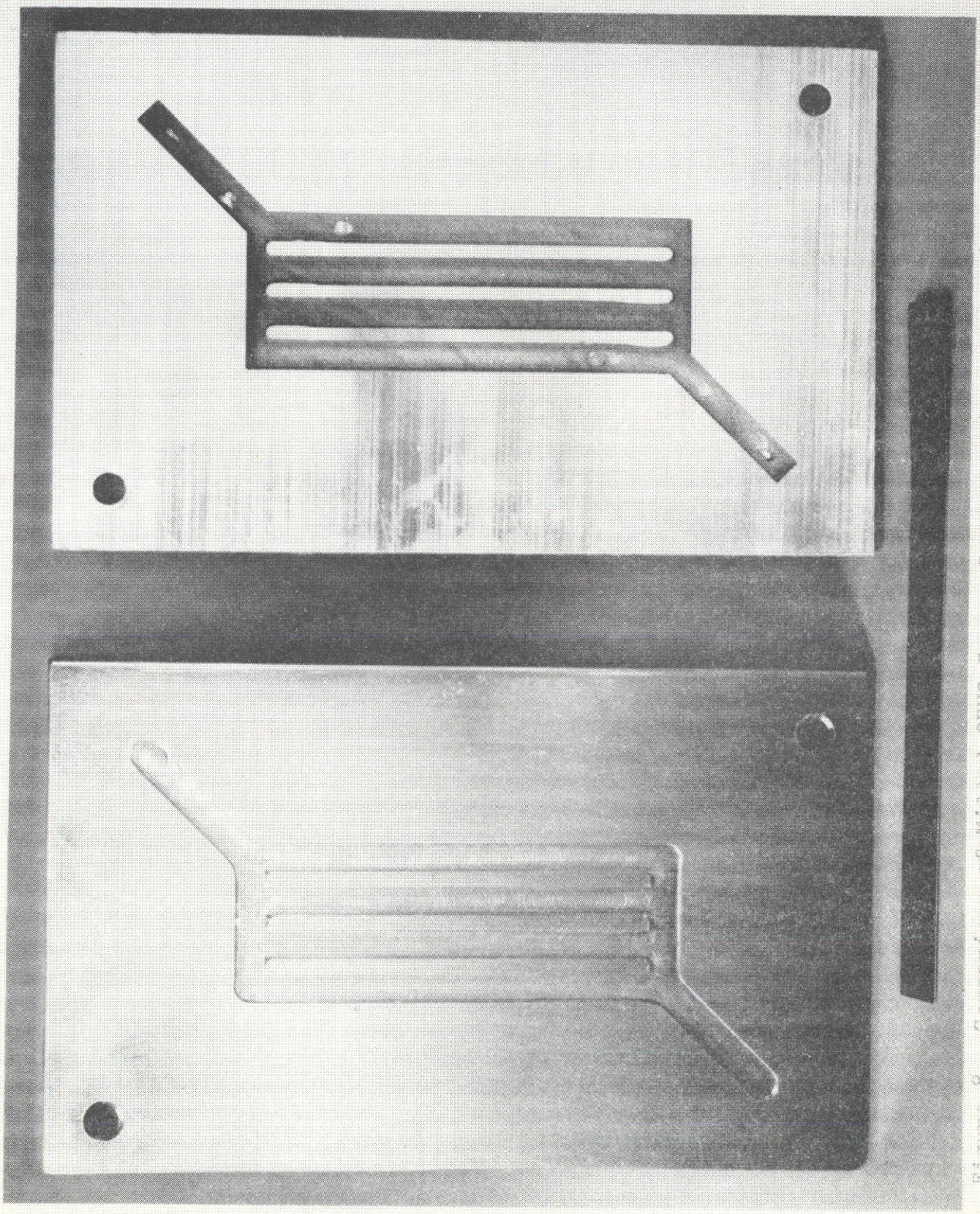

Figure 8. Comparison of Milled OFHC Copper Baseplate (At the left) and Electric Discharge Machined OFHC Copper Baseplate (At the Right)

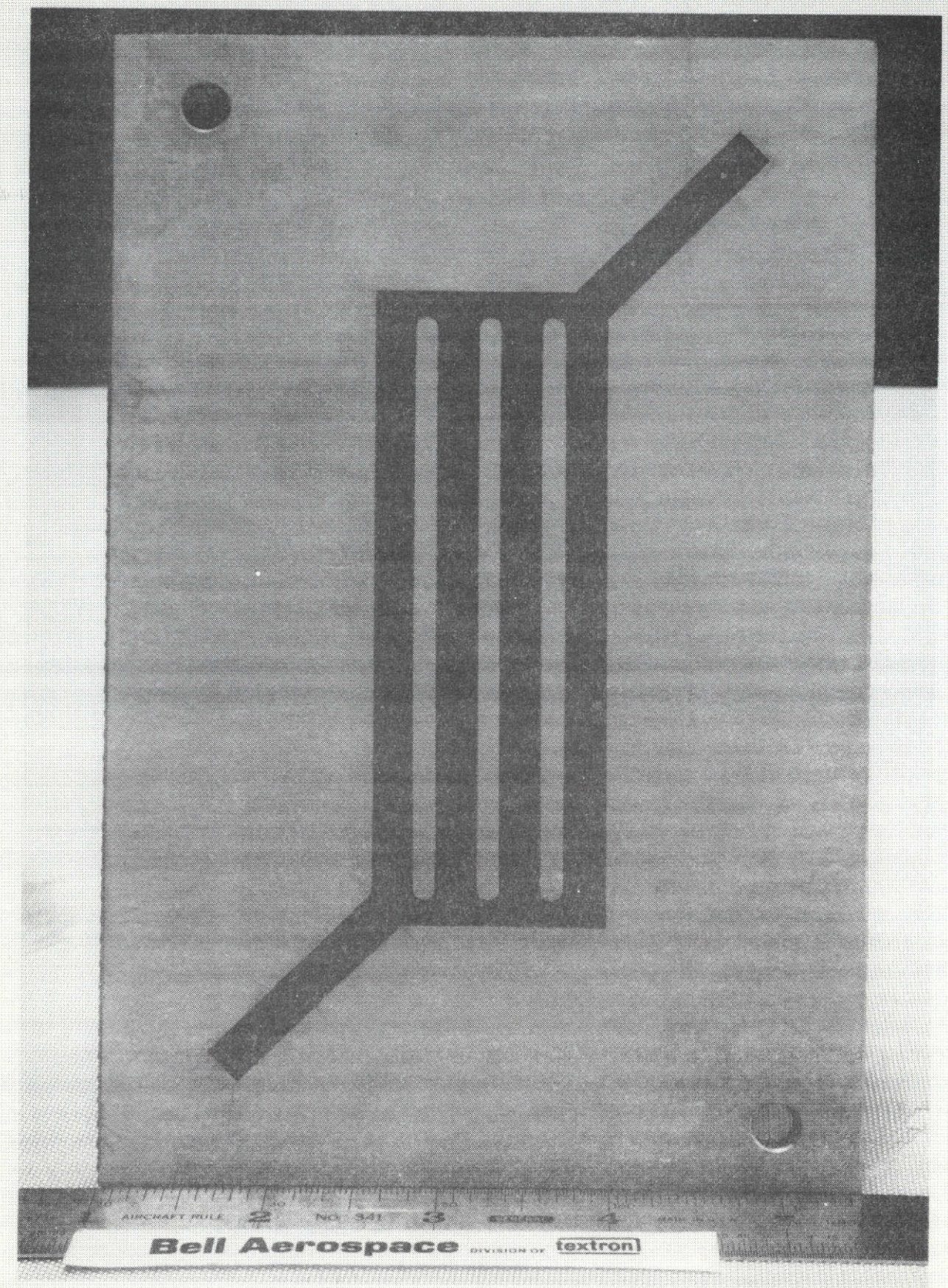

Figure 9. Typical Electric Discharge Machined Nickel 200 Baseplate with Wax Filled Channels and Manifolds for Electroforming

Certain Nickel 200 baseplates required special patterns for use as NDE standards in the equipment calibration work of Task III. Nonbond areas of various sizes, not requiring intimate contact between coverplate and baseplate, were produced by electric discharge machining. Examples of such panels are described in Appendix Section B. Figure 10 illustrates a typical nonbond defect pattern produced in a baseplate for a test standard panel.

2. Preparation of Baseplates for Electroforming

The machined baseplates were dimensionally checked for thickness after all oxides, recast metal and cold work were removed by chemical etching. Measurements of surface flatness were made to assure that resulting electroformed coverplates would be of uniform thickness within a tolerance of ±0.0762 mm (0.003 inch) after final surface finishing. This data appears on the test panel records in the appendix pages of this report.

The baseplates were masked on the backside with plater's tape and fixtured on conductive hangers for electroplating the initial bond layer on the base metal. Before plating, the channel and manifold passages were filled with a plater's wax. This wax was scraped to provide a smooth finish, level with the edges of the lands (bonding ribs). Excess wax was removed by solvent wiping, followed by alkaline detergent cleaning with a scrub brush.

3. Electroforming Nickel Coverplates on Nickel 200 Baseplates

The Nickel 200 baseplates, prepared as previously described, were fully bonded with a layer of electroformed nickel approximately 0.006 mm. (0.00025 in.) thick. The full bond was produced by anodically cleaning the Nickel 200 in a 25 percent by volume solution of sulfuric acid in water. Anodic current at 465 amps/m.^{2} (50 amps/ft.^{2}) of panel surface was used. This was followed by cathodic cleaning and activation in a separate solution of 25

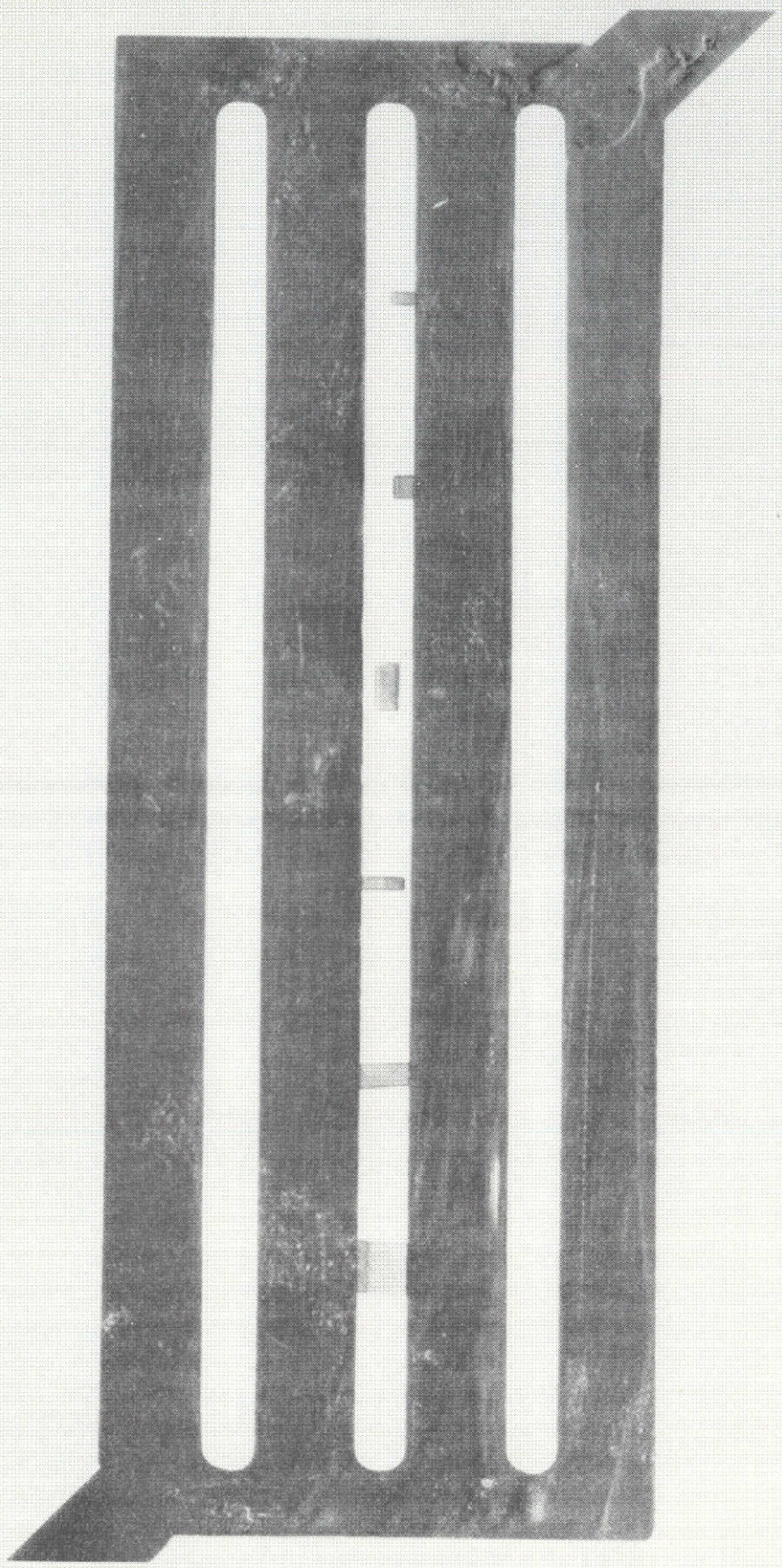

Figure 10. Baseplate for a Calibration Standard Panel with Planned Nonbond Defects Produced by Electric Discharge Machining

percent by volume sulfuric acid in water. The cathodic current was 930 amps/m.^{2} (100 amps/ft.^{2}) of panel surface. The panel was then immersed (with applied cathodic voltage) into the electroforming solution and plated for 15 minutes to obtain the thin full bond nickel layer.

Each panel was rinsed, alkaline scrub cleaned, and dried. If required, planned defect patterns were applied. This was accomplished by masking the face of the panel with plater's tape, leaving the planned defect exposed. For weak bonds, the panels were immersed in the electroforming solution with no current applied. After two to three minutes, current was applied to the panels (cathodes) for a period of four minutes. The current was then interrupted for eight to ten minutes to create a lamination over the weak bond area. The current was reapplied and electroforming continued for ten minutes to produce the planned defect. All electroforming during this process was at a current density of 279 amps/m.^{2} (30 amps/ft.^{2}). Electrolyte operating conditions were as described in Table VI.

Planned nonbond defects were produced by chemically passivating the exposed bonding surface. The passivation was accomplished by immersing the masked panel in a sodium dichromate solution at a temperature of 322°K (120°F) and applying a cathodic current at one ampere for 60 to 90 seconds. The concentration of sodium dichromate in this solution was 35g./L. and the pH was between 5.5 and 6.0 (electrometric). The passivated area was scratched at each end to provide a full bond anchor for subsequent electroforming. The planned nonbond defect was then covered by electroforming with nickel to a thickness of 0.006 mm. (0.00025 inch).

At this stage all baseplates could be treated as full bond panels since the planned defects, where required, were encapsulated under a thin layer of nickel electroform. The next step was to make the wax filled channel surface conductive. On initial

panels, this was accomplished by spraying the panel surface with silver produced by the chemical reduction system using silver nitrate and an organic reducing agent such as fomaldehyde. The fragile nature of the silver conductivizing film resulting from this method often led to porosity in the coverplate. Anodic/cathodic cleaning and activation of the nickel bonding surfaces was too severe for the silver and voids would occur. An improved technique of applying a conductive layer over the wax was needed.

A finely comminuted silver brazing powder was evaluated for conductivizing the wax surfaces. This material (Englehard Silver Power, Type G-3) was rubbed into the wax surface and found to withstand subsequent processing operations without generating voids and porosity.

The conductivized panels were mounted on an electroforming fixture, Figure 11. Plastic frame shields were affixed over the panels to minimize edge build-up effects during electroforming. The anodic-cathodic activation previously described was applied to the fixtured panels and they were immersed in the nickel sulfamate electrolyte (with applied cathodic voltage) to commence electroforming.

Electroforming was performed at an electrolyte temperature of 314°K (105°F) and a current density of 279 amp/m.^{2} (30 amp/ft.^{2}). The fixture containing the panels was rotated at approximately twenty revolutions per minute. Electrolyte was pumped through spray nozzles to flush hydrogen bubbles from the electrodeposited surface. The electroforming rate was approximately 0.0254 mm (0.001 inch) per hour. The coverplates were intentionally electroformed to an excessive thickness to permit machining to a uniform final thickness.

Several panels required coverplates of different material strength. The sequence of operations for these panels was the same, except that current density was adjusted to 651 amp/m.^{2} (70 amp/ft.^{2}).

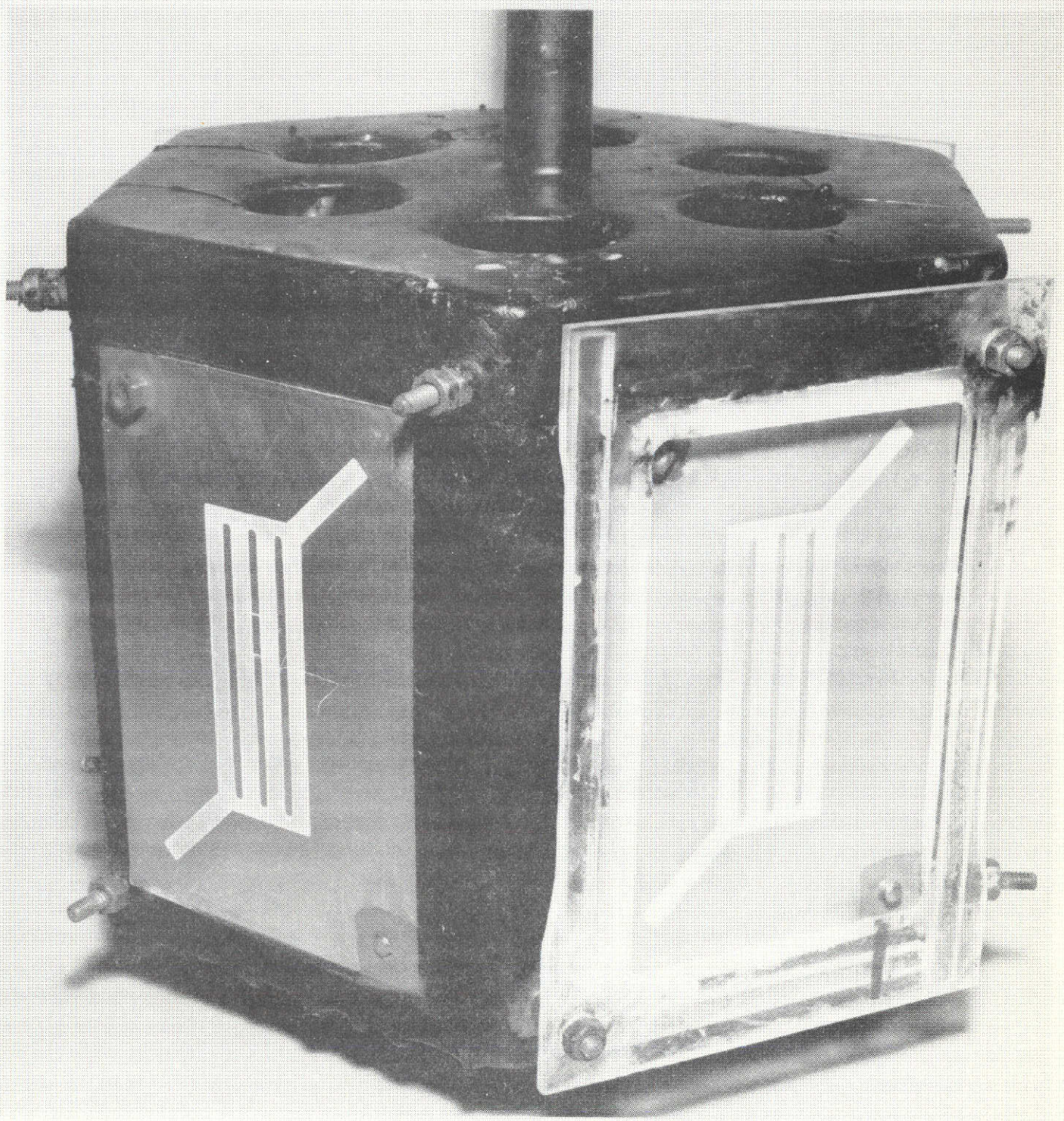

Figure 11. Electroforming Fixture with Panels
(Shield Attached to Panel at the Right)

4. Electroforming Nickel Coverplates on OFHC Copper Baseplates

OFHC copper baseplates were etched in the same manner as the Nickel 200 plates. Dimensional data was recorded after recast metal and oxides were removed. Channel filling and masking was performed according to procedures described for Nickel 200.

Pieces of plater's tape were cut to the size of the defect pattern to be applied (where defects were required) and affixed to the baseplates at appropriate locations. The plates were then alkaline scrub cleaned and immersed in a bright dip solution of 25 percent sulfuric acid in water at room temperature. Immersion was for three minutes. The panels were then drained and immersed with low applied voltage into the nickel sulfamate electrolyte. Low current was initially applied for two minutes to prevent edge burning which leads to poor adhesion of nickel on copper. The current density was adjusted to 279 amp/m.^{2} (30 amp/ft.^{2}) and a fully bonded layer 0.006 mm. (0.00025 in.) thick was deposited in approximately fifteen minutes.

The tapes covering the planned defects were removed. For nonbonds, the sodium dichromate passivation process was applied after the planned full bond area was masked with tape. For weak bonds, the full bond area was tape masked and the planned defect region allowed to oxidize in air overnight. The oxidized area was then nickel plated to a thickness of 0.006 mm. (0.00025 in.) with no cleaning or other preparation prior to plating.

After the above operations, the OFHC copper panels were covered with nickel. Final build-up with nickel was accomplished in the same manner as described for Nickel 200 baseplates.

5. Electroforming Copper Coverplates on OFHC Copper Baseplates

Baseplate preparation was identical to that used for OFHC copper plates on which electroformed nickel was to be deposited. Planned defects were masked in the same way. Sodium dichromate passivation was used to create nonbonds and exposure to atmospheric oxidation employed to produce weak bonds. A thin layer of copper was deposited over the defect to encapsulate it, and the masking was removed from the surrounding full bond area. The panels were then scrub cleaned for final electroforming.

Each panel was mounted on a masked flat fixture with electrical contracts. All panels were activated for bonding the subsequent electroformed copper required to achieve final coverplate thickness. This activation consisted of a three minute immersion in a 25 percent solution of sulfuric acid at room temperature. The fixtured panels were removed from this solution, drained and transferred to the acid copper electrolyte with applied cathodic voltage. The electrolyte was operated at the parameters shown in Table VII. Current density was adjusted to the requirements necessary to produce the desired coverplate strengths.

During nondestructive evaluation of the electroformed copper panels in the equipment limitations investigation (Task IV), it was noted that high acoustic emission counts were obtained in planned full bond areas on several panels. Destructive testing revealed these regions to have weak bonds.

These unplanned weak bonds were almost always in one end of the panel. This led to the conclusion that the sulfuric bright dip was causing a contamination problem. All panels had been allowed to drain to remove excess sulfuric acid from the dip. The draining allowed copper salts to accumulate in the lower portion of the panel. Since some panels were mounted upside-down with respect to identification number, the contamination would occur at either end of the panel with respect to position for testing.

This was proven correct by fabricating a special panel (Panel C-23 C, Appendix Figure C-46) in which the processing sequence was identical to that used on the other panels, except that a thorough distilled water rinse was used after the sulfuric acid bright dip. This panel exhibited no acoustic emission count in the planned full bond area and the bond did not fail below the pressure anticipated to fail the panel.

6. Finishing of Electroformed Coverplate Panels

Pressurization port openings were drilled to provide means of removing the wax from the channels. The wax was removed in boiling water and any residual wax was dissolved by immersion of the panels in trichloroethylene.

The coverplates were machined to the desired final thickness using a single edge cutting blade ("fly-cutter"). It was found that this method of finishing was satisfactory on all panels, except those with electroformed nickel coverplates of less than 0.762 mm. (0.030 in.) thickness. The nature of electrodeposited nickel at thicknesses less than 0.762 mm. resulted in cutting tool wear and tearing of the nickel sufficiently to cause leakage on some panels. This was corrected by machining to an over-thickness and finishing to the final thickness by surface grinding.

All panels were acid etched to remove surface cold work and residual conductivizing silver from the channel passages. Figure 12 illustrates typical test panels as electroformed and after final machining. Holes were drilled in the panels to mount the pressure fittings.

7. Fabrication of Brazed Panels

All OFHC copper baseplates were alkaline cleaned, degreased and acid etched to remove oxides, Figure 13. Baseplate thicknesses were recorded. The plates were drilled to provide reference holes for coverplate alignment prior to brazing. These

Figure 12. Typical Test Panels as Electroformed (Left) and After Final Machining (Right)

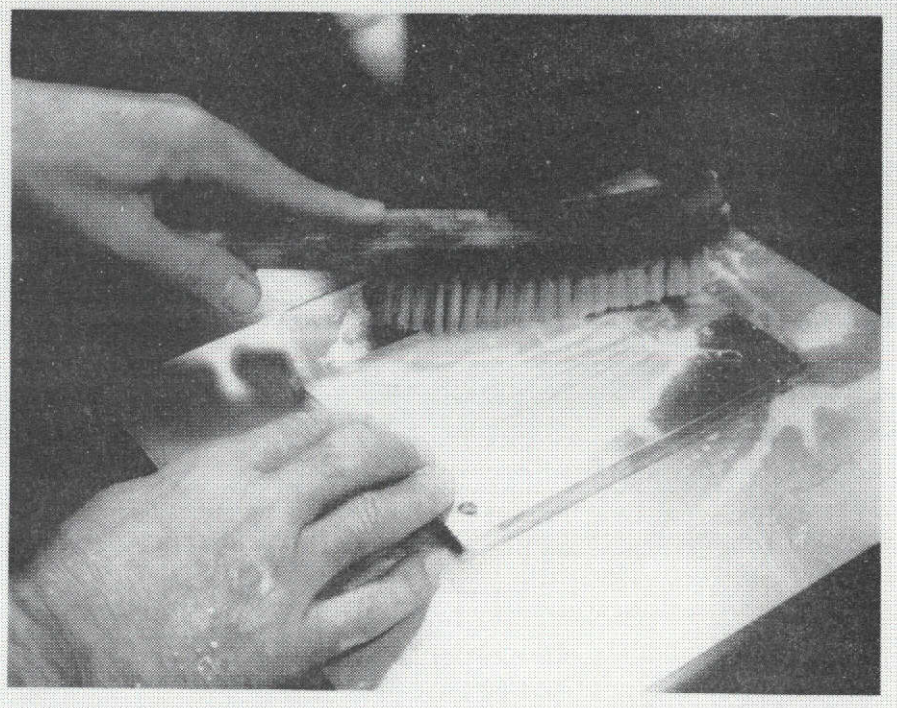

Figure 13. Scrub Cleaning OFHC Copper Baseplates

Figure 14. Cleaning Braze Alloy Prior to Pattern Cutting

holes were in corners where no interference with pressure fittings or test procedures would result.

The type BAg-18 braze alloy was scrub cleaned after acetone degreasing Figure 14. The alloy was final rinsed in distilled water and dried. An acetate template for each baseplate was cut to include the channel/manifold pattern. A separate overlay template was cut to identify size and location of any planned defect required. The braze alloy was cut to the desired patterns with a sharp knife, Figure 15. To assure alignment of the braze alloy patterns in the furnace, the individual sections of alloy were spot welded to the OFHC copper baseplate, Figure 16.

Experience with the BAg-18 braze alloy indicated that reliable braze wetting could not be obtained without first plating a thin layer of nickel on the stainless steel coverplate. Omission of this plating generally resulted in a nonbond. This reaction of the braze alloy was used to produce the planned full, weak and nonbonds.

Using the braze cutting template, the pattern for a weak or nonbond was transferred to the matching side of the coverplate by scribing on the stainless steel surface. The stainless steel surface was then masked to cover those areas where no bonding was desired. The stainless steel surface was activated for a full bond nickel plate by anodic treatment in 25 percent by weight sulfuric acid in water at 465 amp/m.^{2} (50 amp/ft.^{2}) for 1.5 to 2.0 minutes. Each coverplate was allowed to hang in the acid for 15 minutes and then placed in a separate sulfuric acid solution (of the same concentration) for cathodic activation at 930 amp/m.^{2} (100 amp/ft.^{2}) for 2 minutes. The coverplate was then plated for about 10 minutes with sulfamate nickel to produce a thin bonded layer which would enhance braze wetting and bonding at planned locations.

Alignment holes had been drilled into the coverplates to match those in the baseplates. The coverplates were aligned with the braze covered baseplates and dowel pins inserted in the matching

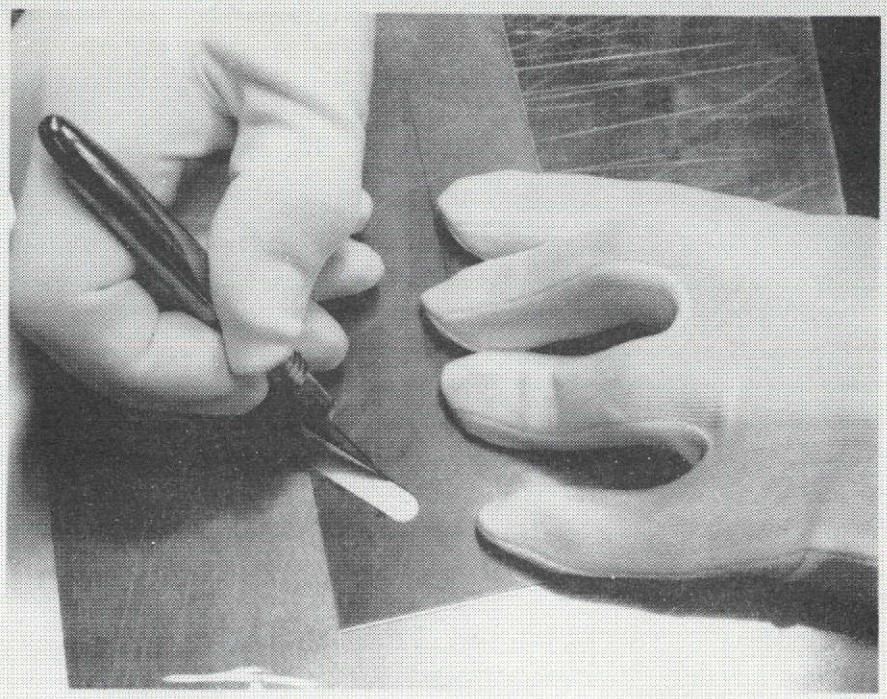

Figure 15. Cutting Braze Alloy Patterns

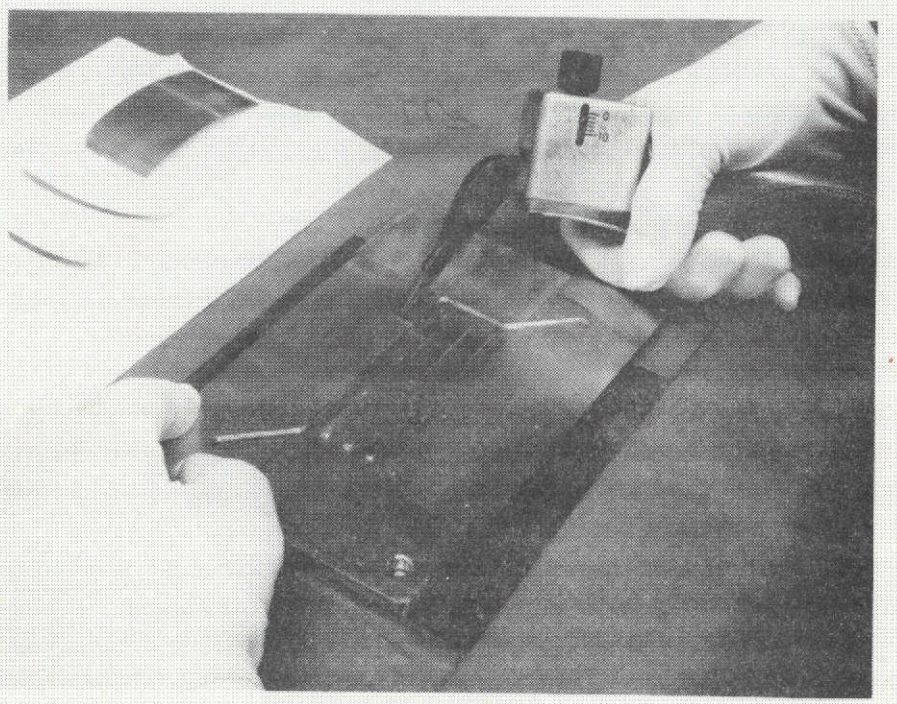

Figure 16. Spot Welding Braze Alloy to Baseplates

holes. The braze furnace was prepared by inserting stop-off coated sheets over the braze fixture plates and panel to be brazed. Thermocouples were inserted, Figure 17, the furnace closed and vacuum applied. When all thermocouples indicated a temperature range of 1044°K (1420°F) to 1055°K (1440°F), the furnace heater was turned off and allowed to cool.

After brazing, the panels were drilled to provide pressurization ports and holes for mounting pressure fittings, Figure 18.

D. TEST CYLINDER FABRICATION

OFHC seamless tube copper was used to fabricate the cylinder liner. The nominal wall thickness was 12.700 mm. (0.50 in.), and the outside diameter was 82.550 mm. (3.25 inches). The liner tube was cut to the length shown in Figure 3 and checked for concentricity. Diameter variations were observed which required machining to a new outside diameter of 81.077 mm. (3.192 inches). The inside diameter was machined at each end of the cylinder to provide accurate centers for any lathe machining later required on the test piece.

Channels and connecting manifolds were machined into the outside surface of the liner in accordance with Figure 3. Holes were drilled and tapped to provide threaded mountings for pressure fittings on the inside surface of the cylinder. This provided pressurization capability at locations which would not interfere with transducer positioning during acoustic emission testing. Figure 19 shows the liner in the machined condition.

The liner was alkaline scrub cleaned, fixtured on a shaft for rotating during electroforming, and waxed to fill the channels and manifolds with inert material. Excess wax was removed and the outside surface was solvent wiped to assure the areas to receive bonds were clean, Figure 20.

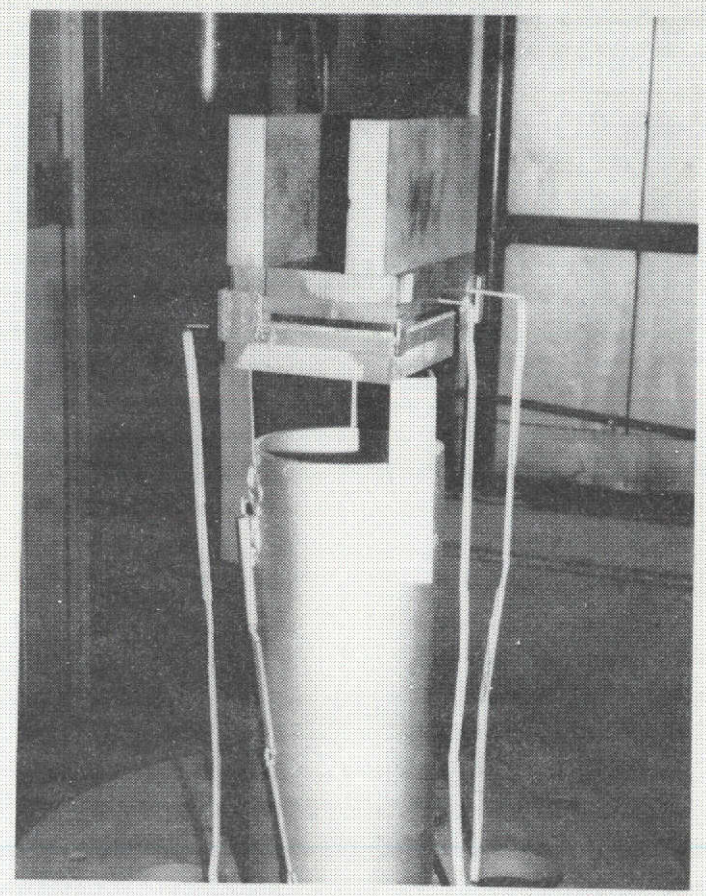

Figure 17. Brazing Fixture and Thermocouples

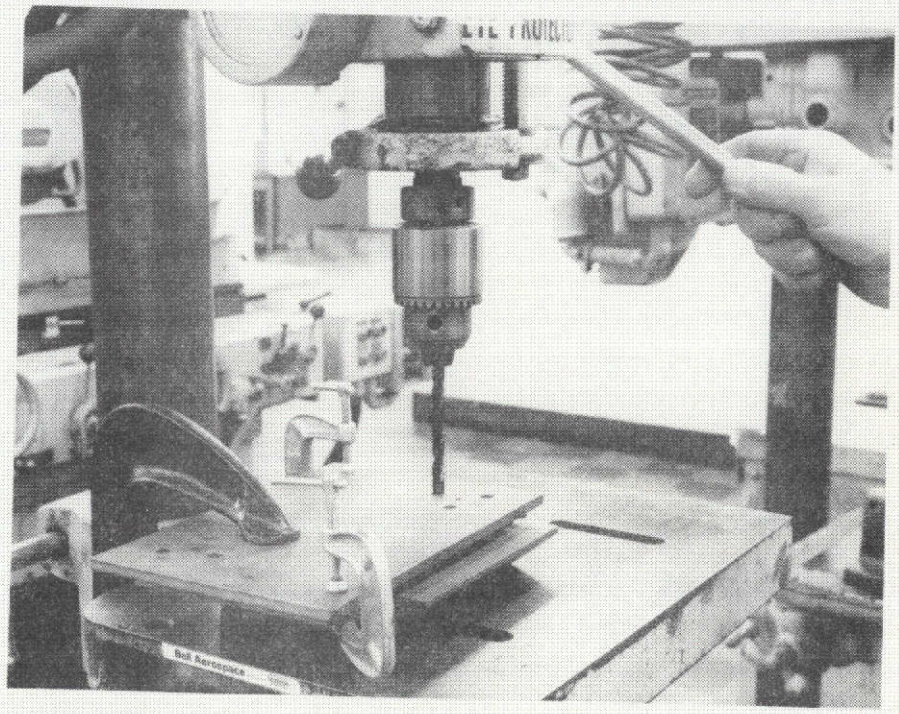

Figure 18. Drilling Pressure Fitting Bolt Holes

Figure 19. OFHC Copper Liner After Machining

Figure 20. OFHC Copper Liner Fixtured and Waxed for Electroforming (Note: Position of Planned Defects)

An initial thin layer of fully bonded nickel was electrodeposited on all exposed OFHC copper surfaces, except for the two areas to receive planned defects shown in Figure 4. These areas were masked during the initial electroplating. The weak bond and nonbond flaws were produced by previously described means. The entire cylinder was then electroformed to a thickness exceeding the required outer shell thickness of 1.016 mm. (0.040 inch) to permit machining for uniformity. A current density of 279 amp/m.^{2} (30 amp/m.^{2}) was employed and the electrolyte operating conditions were those used to produce high strength electroformed nickel on flat panels. Figure 21 shows the cylinder after electroforming.

The cylinder was machined to provide the required outer shell wall thickness. Additional electroforming was applied to the lower portion of the cylinder to increase wall thickness to 1.143 mm. (0.045 inch). This was done to increase buckling strength of the planned nonbond defect to prevent failure of the cylinder before acoustic emission analysis of the planned weak bond could be completed.

E. BOND STRENGTH VERIFICATION PANEL TEST RESULTS

Fabrication and test records for the bond strength verification panels are shown in Appendix Section A. The actual bond strengths were calculated from the formula:

$$\text{Bond Strength} = \frac{\text{Pressure (Failure)} \times \text{Total Channel Width}}{\text{Width of Land}}$$

Where: Total channel width is the combined width of both adjacent channels.

Table XI lists the calculated bond strengths.

Figure 21. Fixtured Test Cylinder After Electroforming

TABLE XI - CALCULATED BOND STRENGTHS FOR BOND STRENGTH VERIFICATION PANELS

Panel No.	Material Combination		Bond Type	Bond Strength	
	Baseplate	Coverplate		MN/m^2	kpsi
N-08	Nickel 200	EF Nickel	Full	276+	40.0+
N-07	Nickel 200	EF Nickel	Weak	198	27.2
N-20	Nickel 200	EF Nickel	Weak	193	28.0
N-05 "A"	Nickel 200	EF Nickel	Nonbond	55	8.0
C-07N	OFHC Copper	EF Nickel	Full	276+	40.0+
C-13N	OFHC Copper	EF Nickel	Weak	110	16.0
C-14N	OFHC Copper	EF Nickel	Weak	102	14.8
C-15	OFHC Copper	EF Nickel	Nonbond	83	12.0
C-02C	OFHC Copper	EF Copper	Full	255	37.0
C-05C	OFHC Copper	EF Copper	Weak	74	10.8
C-10C	OFHC Copper	EF Copper	Weak	152	22.0
C-11C	OFHC Copper	EF Copper	Nonbond	42	6.0
B-03	OFHC Copper	Brazed S.S.	Full	110	16.0
B-07*	OFHC Copper	Brazed S.S.	Weak	146	21.2
B-10	OFHC Copper	Brazed S.S.	Weak	51	7.4
B-05	OFHC Copper	Brazed S.S.	Nonbond	33	4.8

* Panel B-07 actually contained a full bond.

+ Indicates that the bond did not fail at 69 MN/m^2 (10 kpsi).

The bond strengths reported for nonbonds were due to coverplate buckling resistance.

V. TASK III - NDE EQUIPMENT CHARACTERIZATION AND CALIBRATION

NDE standard panels were fabricated in Task II to be used to establish baseline characterization and calibration for the NDE methods to be applied in the program. The three basic methods to be used are those found most feasible under Contract NAS 3-14376. These are ultrasonic "C" scan, holography and acoustic emission.

A. ULTRASONICS

Three basic methods of ultrasonic testing were comparatively evaluated for nonbond detection capability. These methods were:

1. Pulse echo longitudinal wave which introduces the sound normal to the entry surface and is therefore oriented to detect delamination and bond defects parallel to the entry surface.

2. Through transmission which uses two transducers (one transmitter and one receiver) located on opposite sides of the specimen under test. It also is suitably oriented for delamination type defects.

3. Reflector method which is similar to the through transmission method with the exception that a smooth surface replaces the receiving transducer and this acts as a reflector, returning the sound back to the transmitting transducer. This technique is particularly useful on thin materials in which the front and back surface signals cannot be readily separated on the scope (cathode ray tube).

All three methods are shown schematically on Figure 22. In order to obtain controlled comparative results, a standard was designed with "defects" in pairs, separated by distances corresponding to the

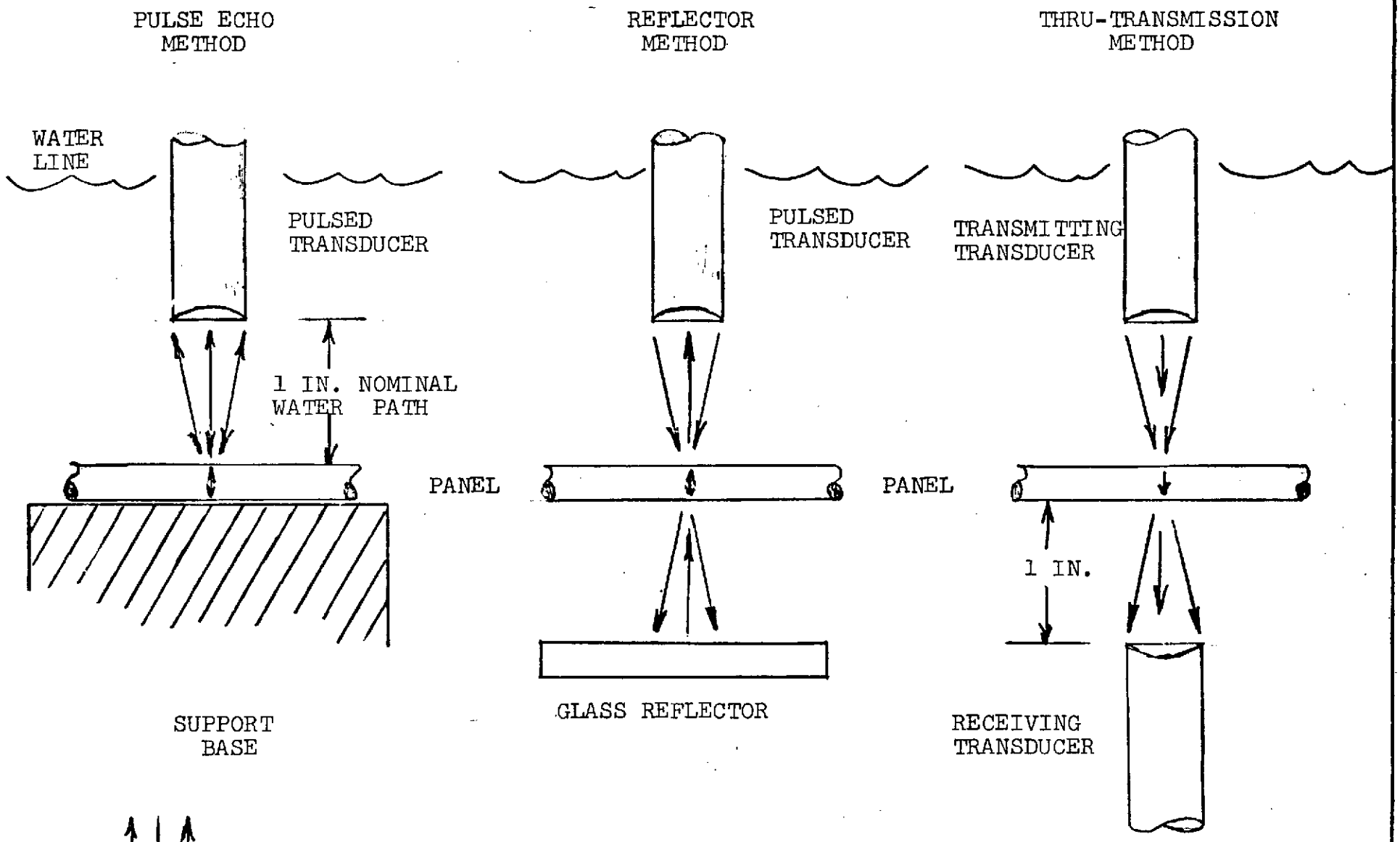

Figure 22. Schematic Diagram of Ultrasonic Methods

land width and decreasing fractions thereof. The actual dimensions are shown on page 36 of the Appendix. This pattern was then ultrasoncically evaluated on similar panels with different electroform coverplate thicknesses. The optimum results obtained by each of the methods are shown in the Appendix on Pages 37, 39 and 41. An analysis of these results shows that through transmission appears to have only limited application since it is inferior to the pulse echo method on thick panels, i.e.-1.018 mm (.040 inches) or greater, and to the reflector method for very thin build-ups. The optimum pulse echo technique consisted of utilizing a 20 MHZ medium focused Parametrics transducer with a 50W pulse-receiver. This technique appeared to be more ideal for the 1.018 mm (.040 inch) coverplate, which was finally selected for Task IV panels based on bond strength test experience. This method could detect two 0.10 mm slots separated by 0.15 mm. Individual slot resolution was not attained however.

The optimum reflector equipment was a 10 MHZ medium focused transducer and a 10N pulse receiver.

Utilizing the parameters established above, two series of tests were made to establish any enhancement attainable by conducting the ultrasonic test with the panel pressurized internally — the theory being that internal pressure would increase the defect "separation", thus making it a more ideal reflecting surface. Another standard was produced to contain defects which did not completely bridge the land width (considered a more severe case for ultrasonic detection). No beneficial results were obtained from pressurization as high as 3.11 $MN/m.^2$ (450 psig), and at this point the work was stopped since higher pressure would have affected acoustic emission results in Task IV panels. The results are presented on Page 43 of the Appendix.

One further aspect of ultrasonic testing was also evaluated during this task - that of high resolution equipment. Candidates considered included complete instrument packages, special transducers and new experimental type approaches. The most

significant gain from this work was the introduction of the Parametrics 20 MHZ transducer for the pulse echo test. This innovation decreased the minimum thickness inspectable by the pulse echo method to 1.08 mm. (.040 inch).

The other promising approach was the use of first interface reinforcement technique for thin materials. This is shown in Figure 23. The approach consists of monitoring the first interface signal to detect and record surface conditions (note: machine marks in the figure) and then reinforcing this signal with the second interface. This is achieved by selecting the transducer frequency, focal length, water path, normalization, gain and pulse length which causes the second interface peak to exceed the first. The difference is then gated. Although showing improved resolution, the method is extremely operator sensitive and also requires thin, smooth and parallel surfaces for best results. All of these factors led to its exclusion from further study for this program.

B. HOLOGRAPHY

A similar approach as used in the ultrasonics evaluation was taken to evaluate stress means and holographic techniques. Since the "nonbond" is the simplest defect to detect, it was employed to establish relative holographic capabilities and feasibilities based on two different coverplate thicknesses for electroformed nickel standards. Page 44 of the Appendix shows the dimensions chosen and it should be noted that the defects consisted of full land width, half land width and "totally enclosed" voids.

Three types of stressing were evaluated. These were:

1. Heat - front and back faces.

2. Mechanical Vibration.

3. Internal Pressurization.

CRT Display

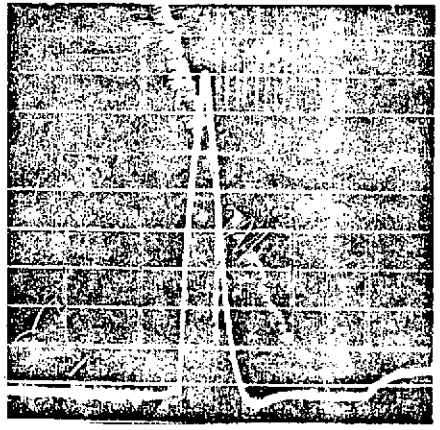

Narrow Recording Level

Signal Increases When Transducer is Directly Over Thinner Member

Standard Panel No. 14
.020" Cover Plate Thickness

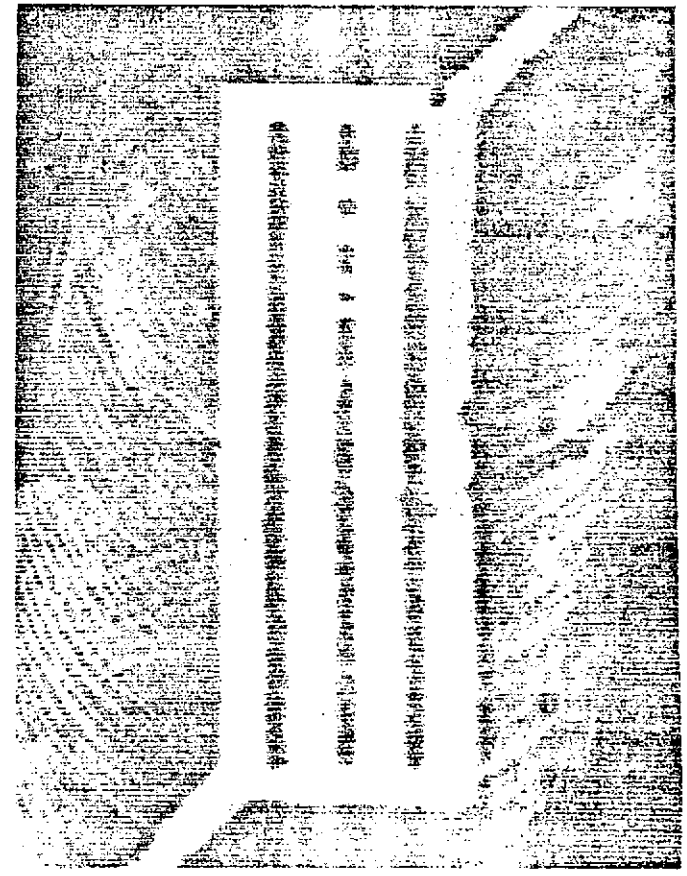

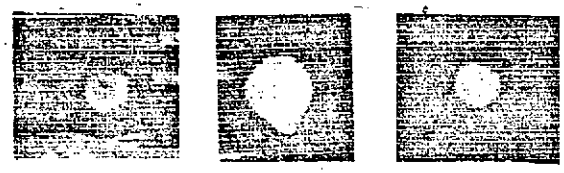

.015" .020" .015"

Metal Travel Flat Bottomed Holes

Note: Machine Mark Pattern

Figure 23. Ultrasonic First Interface Reinforcement Technique

The failure of mechanical vibration to produce results also negated the use of time average holography.

The results of the pressure study using the time-lapse technique are shown on pages 45 and 47 of the Appendix. Several interesting features are shown.

1. The same sensitivity is achievable with lower pressure on the thinner materials. This demonstrates the potential use of holography during the early chamber build-up stage when optimum cost savings can be achieved.

2. For a given size defect, increase in pressure does not enhance detection or size correlation.

3. The smallest readily interpretable unbond common to both thicknesses is a slot 1.57 mm x 1.57 mm (.062 inch) open to pressure on one side.

4. An interesting observation on the thin cover plate at higher pressures is that while small and enclosed voids did not always show clearly in the land, there was usually a dark area or movement associated nearby in the channel area.

Results obtained on the holographic bond strength study of weak bonds were disappointing. This was primarily due to the heavy coverplate thickness used for Task III panels which required pressures in excess of those desired to develop coverplate movement. Also the initial weak bond process produced stronger "weak" bonds than planned. A new Task IV cover thickness was calculated. Nonbond size correlation, Pages 55 and 57 of the Appendix, was excellent with the defects showing actual size.

Only internal pressure was successful in producing interpretable holograms. There was no significant advantage in use of either gas or liquid. For safety reasons, water was chosen to afford a common pressurization media for holography, acoustic emission and burst testing.

The lack of success on heating methods was considered to be the high thermal conductivity causing rapid equalization of stresses in the material. Some changes would be observed during real-time holography. These occurred too rapidly for either visual evaluation or photography. The use of real-time holography was established during this program. Initially, a 15MW laser was in use and very little success was achieved with real-time holography. This laser was replaced with a 50MW laser prior to Task IV. With this equipment, real-time was more clearly defined. It was also possible to photographically record the results. Figure 24 shows the results attained on panel N-38. The comparable time lapse hologram is shown on Page 77 of the Appendix. The results of real-time holography are not as consistant when compared to time lapse technique. The explanation probably lies in the methods of producing the different holograms. In real-time, it is necessary to remove the first exposed hologram for processing and then return it to the film photo holder for viewing and recording of the real-time fringes by photography as they occur. Background fringes almost invariably occur due to such factors as repositioning problems, and emulsion shrinkage. In time-lapse, these problems do not occur since no plate movement or developing occurs until completion of the test. Even with these limitations, real-time proved to be a useful tool during Task IV.for selecting the necessary test pressure. The test was conducted in real-time to establish the pressure, and then a time-lapse hologram was taken at that pressure. This not only eliminates the trial and error method of establishing the test pressure, but also enables immediate shutdown if any unusual pattern should be experienced at low pressures.

AFTER ACOUSTIC EMISSION

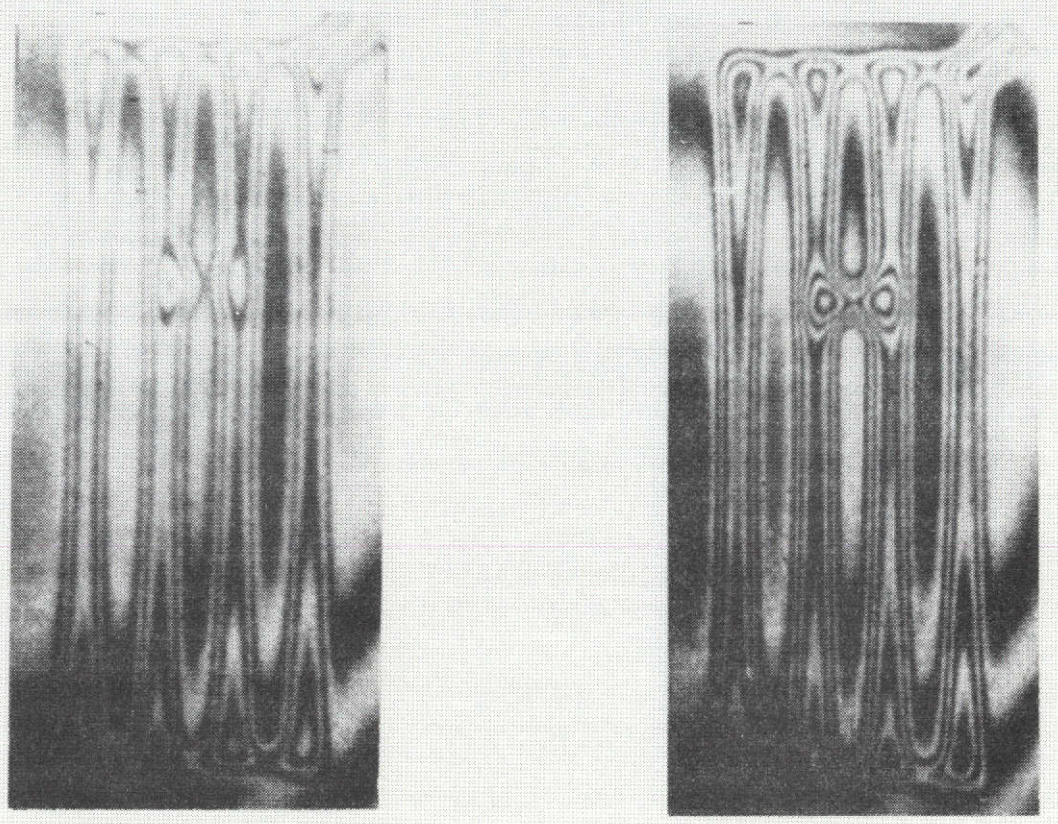

13.8×10^5 N/M^2
(200 PSI)

17.25×10^5 N/M^2
(250 PSI)

Figure 24. Real Time Holography Results for Test Panel N-3B

C. ACOUSTIC EMISSION

The task to characterize flaws and bond strength by standards using electroformed nickel on nickel revealed problems that highlighted panel design limitations. The results do give some positive information in that if the design is such that heavy electroform build-up is necessary, it is essential the NDE is performed at an early stage. The results on Appendix pages 65, 67 and 69 clearly demonstrate that the strength of surrounding material totally dominates the defects and prevents their movement and hence detection. The weak bond samples (Pages 61 and 63 of the Appendix) verified that weak bonds emit more noise than nonbonds. Due to changes made in thickness, it was not possible to establish any relationship between count and strength. In addition, land edge and internal surface condition caused unusual emissions on the full bond and defect location panels. These bond conditions, although not completely "as planned", did assist in the redesign of Task IV panels for coverplate thickness. It was determined initially that the same design was to be used for all material combinations. Since acoustic emission tests had been run for information during Task II, it was considered pertinent to evaluate these results from a nondestructive standpoint to ascertain if acoustic problems or design problems existed in these material combinations also. Figure 25 and Figure 26 show summation versus pressure plots for copper-nickel and copper-copper combinations, respectively. These results show an excellent characterization of the curves. One very significant feature is evident in the copper-copper graph - copper emits very little noise prior to failure making testing difficult nondestructively. It was obvious that the filter and gain used for electroformed nickel were not sufficiently sensitive for copper. Accordingly, it was necessary to remove all filters and increase the gain for all Task IV electroformed copper panels.

An acoustic emission characterization for electroformed nickel on Nickel 200 bonds of various integrities is shown in Figure 27. This was produced using surface flatness specimens (Panels N-13, N-46 and N-42) from Task IV results.

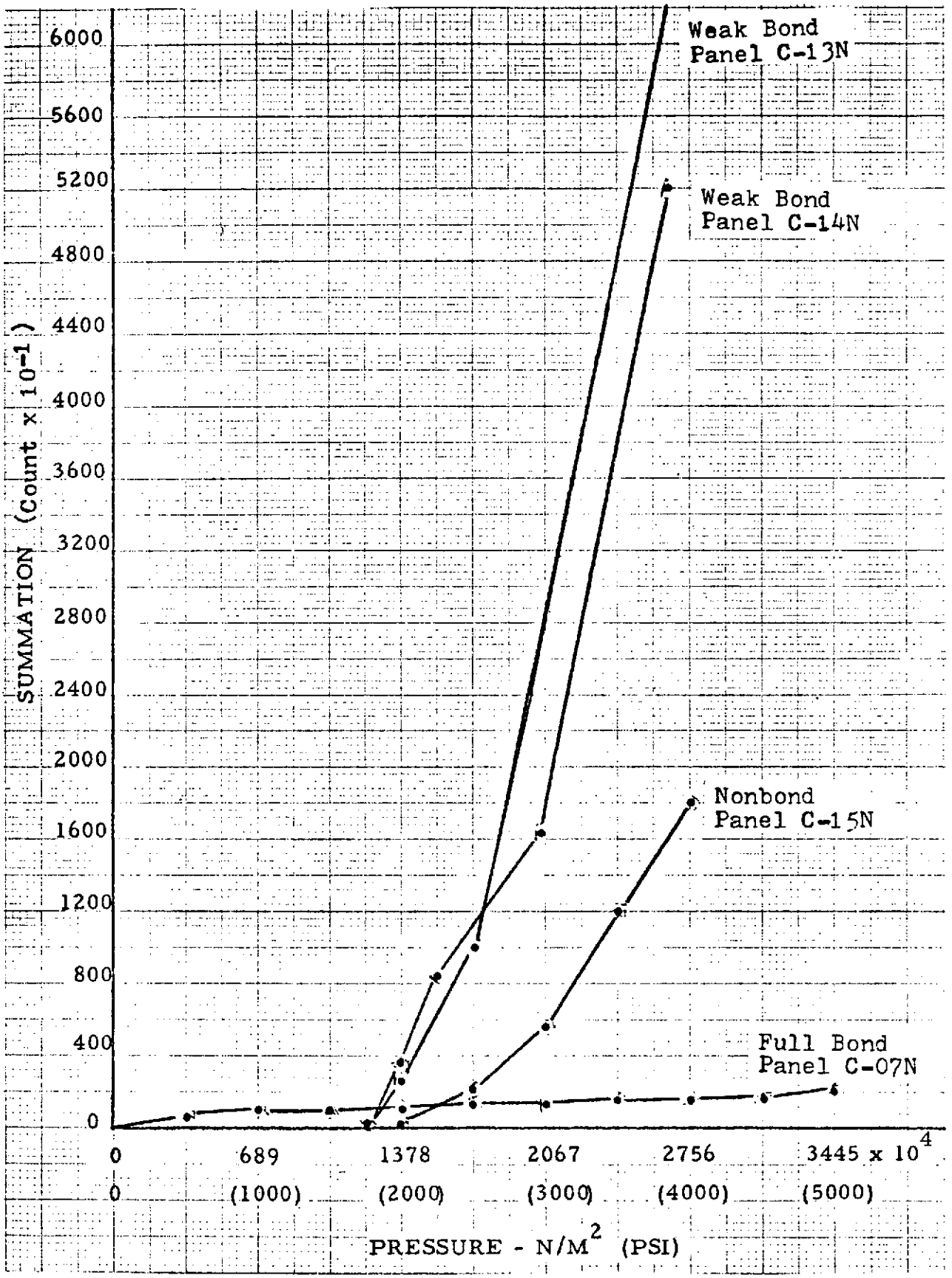

Figure 25. Characteristic Acoustic Emission Curves for Electroformed Nickel Bonded to OFHC Copper

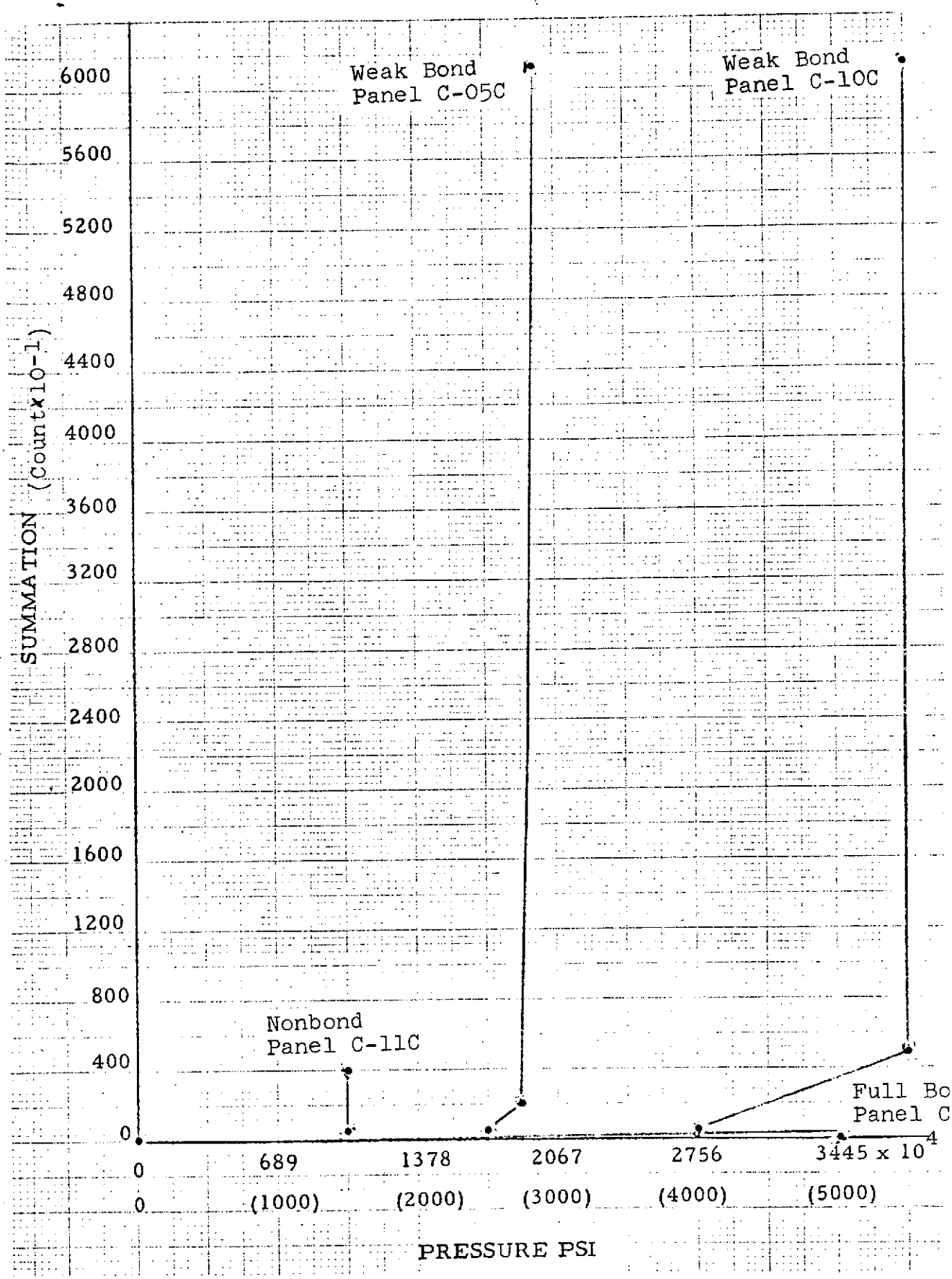

Figure 26. Characteristic Acoustic Emission Curves for for Electroformed Copper on OFHC Copper

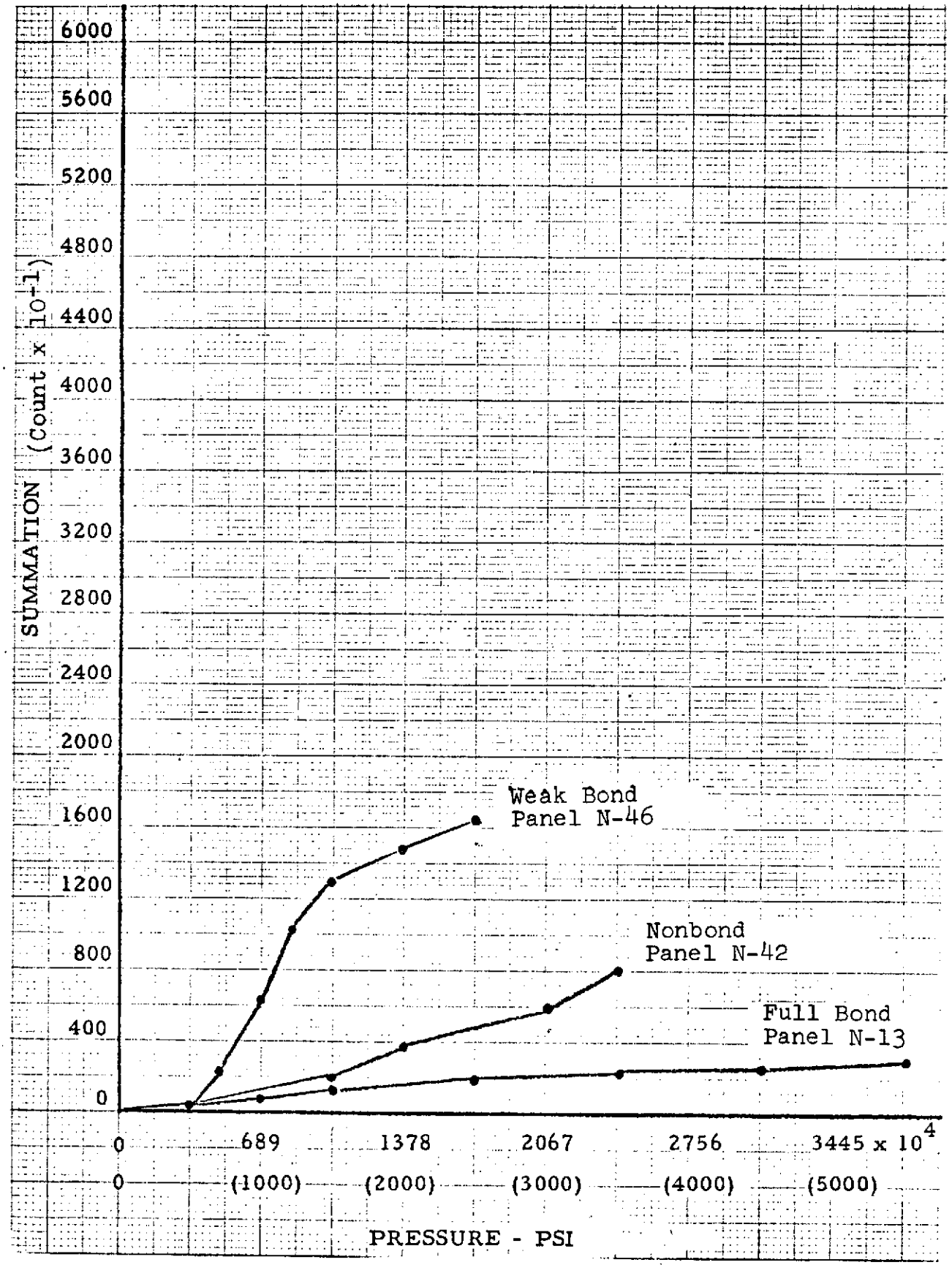

Figure 27. Characteristic Acoustic Emission Curves for Electroformed Nickel Bonded to Nickel 200

Each type of bond integrity responded similarly and comparatively for each material combination with electroformed coverplates.

D. SPECIAL STUDIES

The effect of surface finishing for coverplate flatness was an item of concern due to possible influence of cold work on acoustic emission data. This was evaluated in a special study using full bond panels to eliminate the additional variable of defect noise emission.

Three Nickel 200 baseplates with narrow (1.524 mm, 0.060 inch) lands were electroformed with nickel and surface finished for flatness by three different methods. All panels contained comparable coverplate thicknesses of 1.397 mm. (0.055 inch) after finishing. One panel (Panel N-53) was "as electroformed", except for surface grinding the areas for pressure fittings to the flatness required to prevent leaks. Panel N-54 was machined for flatness, and Panel N-55 was surface ground.

Figure 28 compares the acoustic emission curves for the various finishing methods. Grinding and machining introduced some cold work, but the effect of these operations did not generate an acoustic emission curve outside of the characteristic curve for full bonds.

Another narrow land panel (Panel N-52) was produced with a thin coverplate (0.254 mm., 0.010 inch) and a nonbond, 12.70 mm (0.50 inch) long in the center land. Holograms at different pressures depicted the defect as shown in Figure 29.

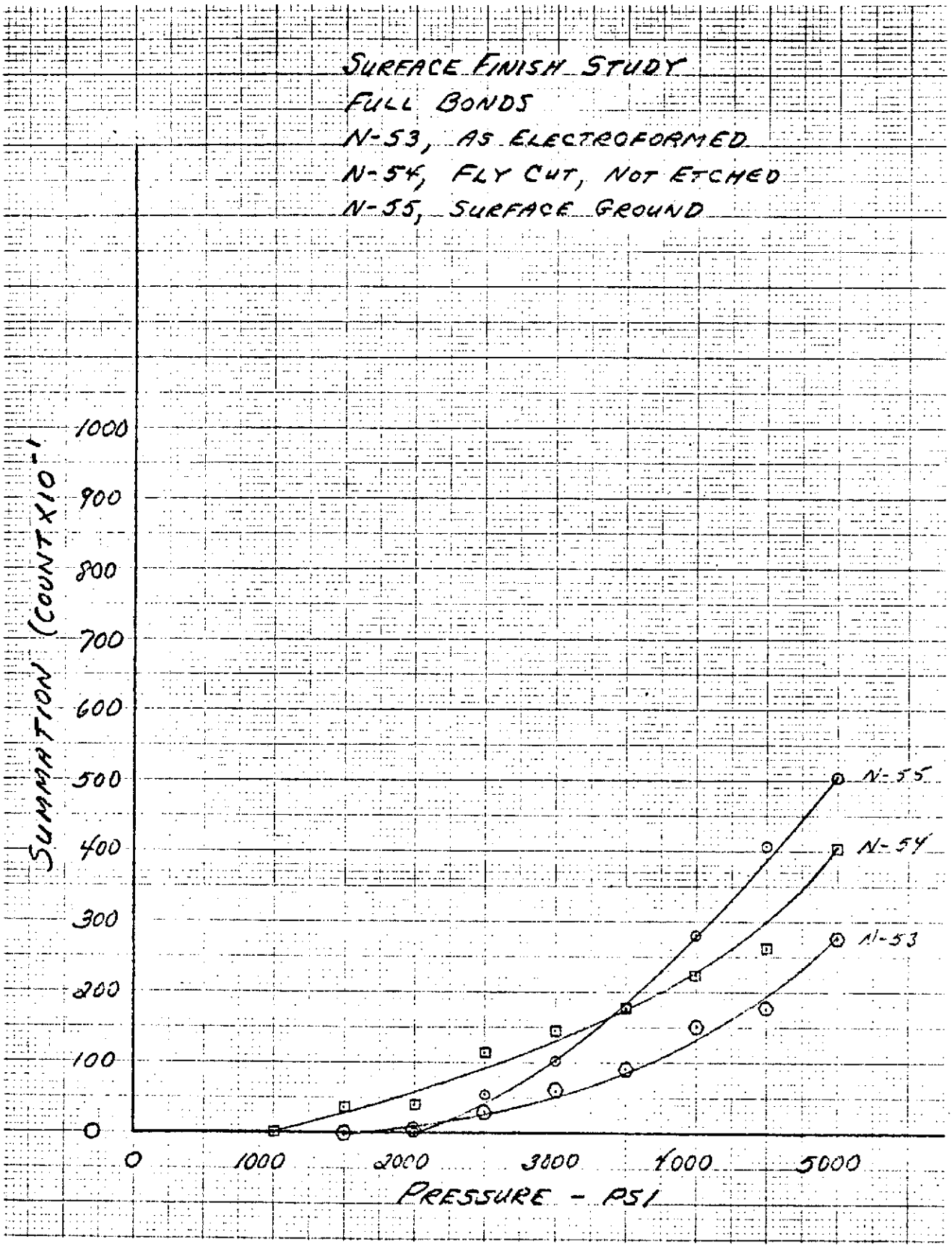

Figure 28. Effect of Surface Finishing on Acoustic Emission Count

FIGURE 29 - HOLOGRAMS OF THIN COVERPLATE PANELS

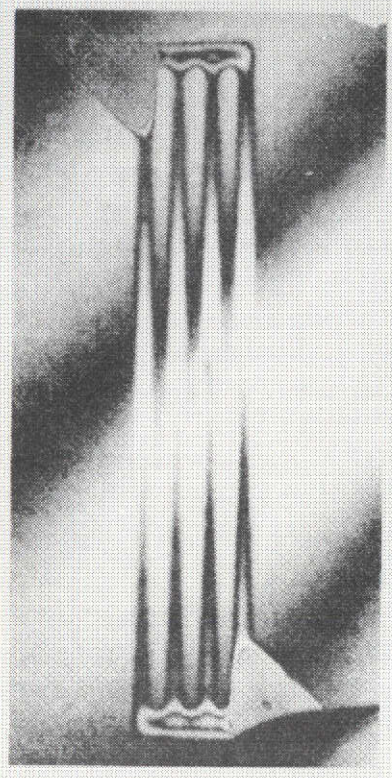

1.7×10^5 N/M^2
(25 PSI)

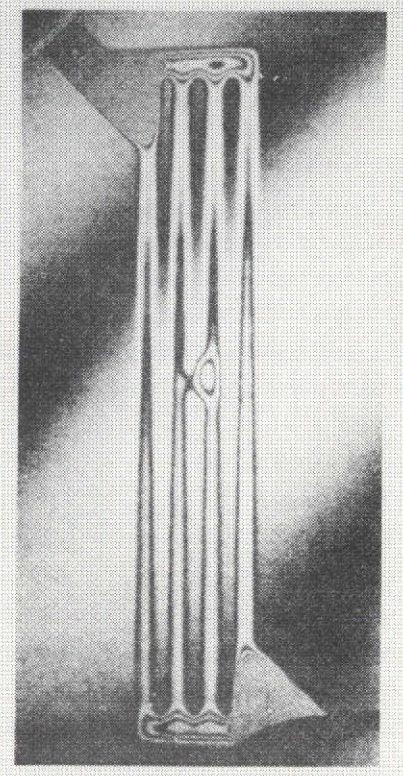

2.07×10^5 N/M^2
(30 PSI)

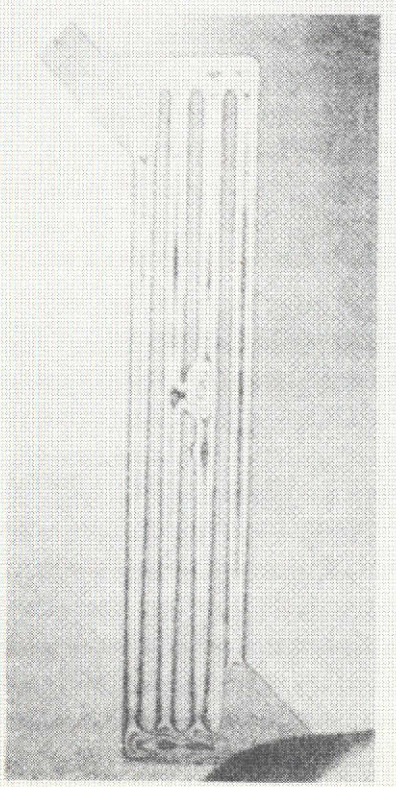

2.76×10^5 N/M^2
(40 PSI)

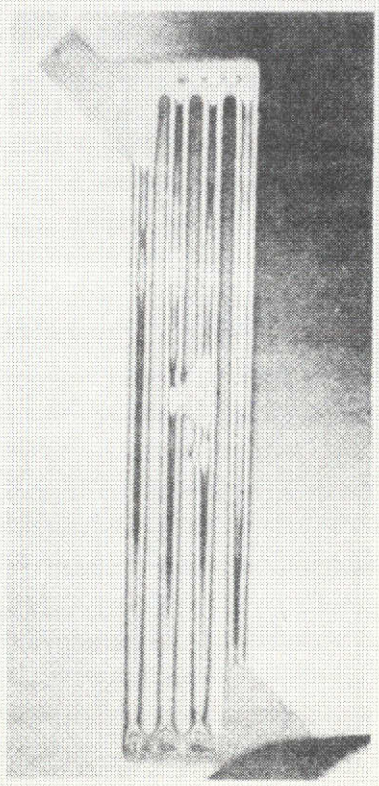

3.45×10^5 N/M^2
(50 PSI)

VI. TASK IV - NDE EQUIPMENT LIMITATIONS INVESTIGATION

Based on the results of Task III, the standard techniques used for equipment limitation evaluation were established. These are shown on Pages 63 through 66.

Section C of the Appendix gives a detailed presentation of the results obtained in Task IV.

During the initial testing on Task IV panels, test sequencing changes and premature failure resulting in lost data was experienced. With the addition of the 50MW laser and hence a real-time holographic capability, the following sequence was established to minimize lost data problems:

1. Ultrasonic "C" scan evaluation (without pressure) to disclose nonbonds, if present.

2. Testing with time-lapse holography at pressure from 100 psi to approximately 300 psi. Actual pressure was established by real-time to avoid unnecessary pressure and possible panel damage.

3. Acoustic emission testing at minimum hydrostatic pressures necessary to cause the emission summation rate to exhibit a noticeable rate change.

Figure 30 shows the test fixture used in performing holographic evaluation. This fixture minimized external stressing and vibrational interferrences.

BAC 1926

DATE N/A
REV. N/A
QUALITY ENGINEERING APPROVAL N/A

Bell Aerospace Company

ULTRASONIC TECHNIQUE NO. N/A

NOTE: † Optional
* Equivalent items may be substituted subject to Quality Engineering approval

PART NAME - NASA Panels
Electroformed, Brazed and
PART NUMBER - Bonded Processes
Part Number
JOINT NO. - 8654-470001

MATERIAL - Nickel, Copper, Stainless Steel

METHOD - Reflector
Immersion

* EQUIPMENT	* TOOLING
Sperry	Automation
721 Reflectoscope	Inds immersion
10N Pulser Receiver	Research Tank with 11"
E550 Transigate	Alden "C" Scan Recording
Special Function	Option
Cabinet containing	
Alden Drive Inter-connect	
and Amplifier	

SCAN PLAN

Scanning 3.0
Direction
Setting
←→
Indexing
Direction 3.0
Setting
↕

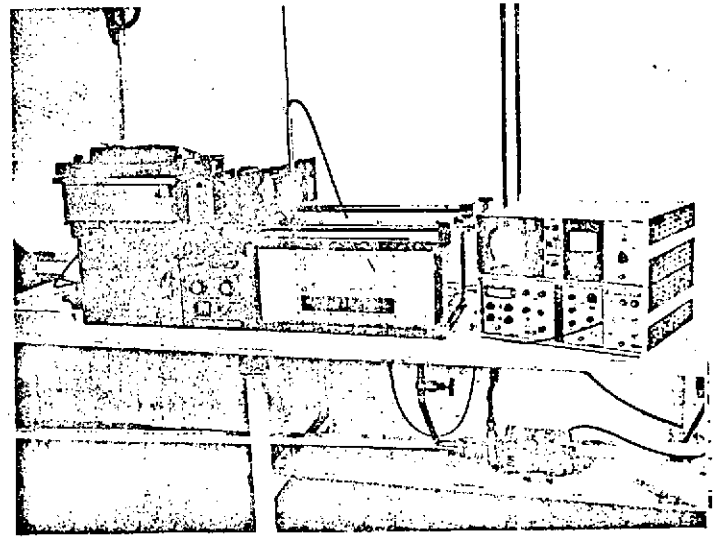

Instrument Settings:
+ Gate, bond interface, 3-6 line threshold level,
Lo Gain, Peaked 10-15 Line Operating Level.

* RECOMMENDED TRANSDUCER TYPE — 3/4" Dia., Medium Focused, 1.5" Focal Point, 10 MHz Freq.

REFERENCE STANDARD CRITERIA

STANDARD NO.	MATERIAL	HOLE SIZE	DEPTH	SHAPE	REMARKS
N/A	Nickel	N/A	.1195" Thick	Flat	Used for normalization and focus control

DATE N/A
REV. N/A
QUALITY ENGINEERING APPROVAL N/A

Bell Aerospace Company

ULTRASONIC TECHNIQUE NO. N/A

NOTE: † Optional
* Equivalent items may be substituted subject to Quality Engineering approval

PART NAME - NASA Panels
Electroformed, Brazed
PART NUMBER - Bonded Processes
PART NUMBER
JOINT NO. - 8654-470001

MATERIAL - Nickel, Copper, Stainless Steel

METHOD - Pulse-echo Longitudinal Wave
Immersion

* EQUIPMENT	* TOOLING
Sperry	Automation
721 Reflectoscope	Inds immersion
50W Pulser Receiver	Research Tank with 11"
E550 Transigate	Alden "C" Scan Recording
Special Function	Option
Cabinet containing	
Alden Drive Inter-connect	
and Amplifier	

SCAN PLAN

Scanning 3.0
Direction
Setting
←→
Indexing
Direction 3.0
Setting
↕

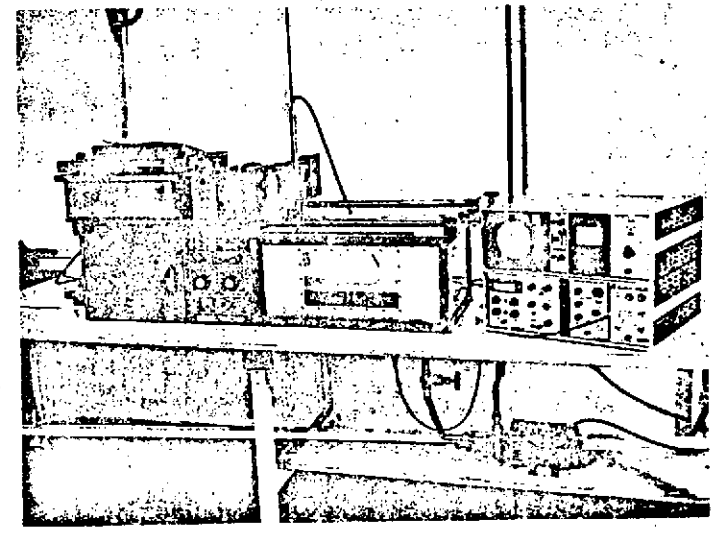

Instrument Settings:
+ Gate, bond interface, 3-6 line Threshold Level,
Lo Gain, Peaked 10-15 Line Operating Level.

* RECOMMENDED TRANSDUCER TYPE — 3/4" Dia., Medium Focus, 20 MHZ Freq. (Panametric)

REFERENCE STANDARD CRITERIA

STANDARD NO.	MATERIAL	HOLE SIZE	DEPTH	SHAPE	REMARKS
N/A	Nickel	N/A	.1195" Thick	Flat	Used for normalization and focus control.

HOLOGRAPHIC INTERFERROMETRY TECHNIQUE
JODON HS-1C SYSTEM

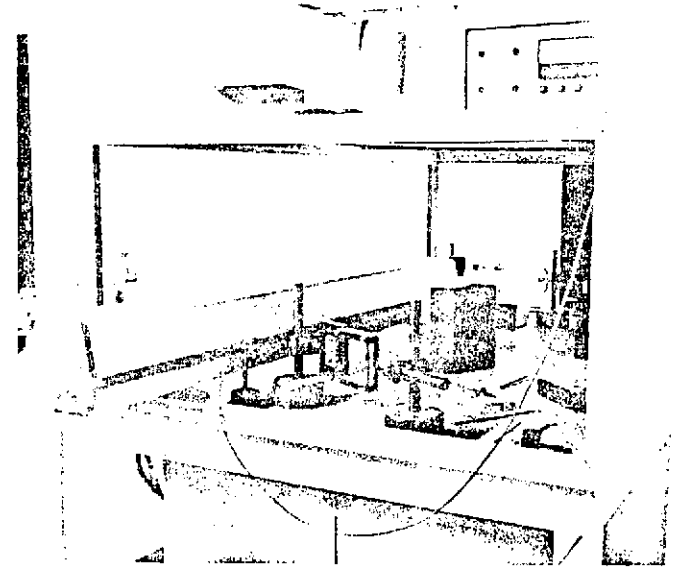

POLAROID CAMERA FACTORS

Type 107 Film.
Close Up Lens.
Inf. Focus.
14 in. Object to Lens Distance
100% Reference
Beam Intensity
F-16 1 Sec Exposure

TEST CRITERIA 1/2 EXP.

Tech: Time-Lapse Time
Mode Integrate Scale Hi
Set 900 Ergs./cm^2 NA Min. Sec.
Vernier 1.8 Beam Coff. 25%
Laser 50 mw Den. 80 mw/cm
Stress Gas-Nitrogen

OTHER FACTORS

105 in. Splitter to Film Plate Beam Distance.
20:1 Ratio Divergence Lens.
7 to 1 Beam Ratio.
30 Avg. Beam Splitter Position.
12 in. Object to Film Plate Distance
2 Min. Dev. at 68°F
1.6 Avg. Density

ELECTRONIC SHUTTER

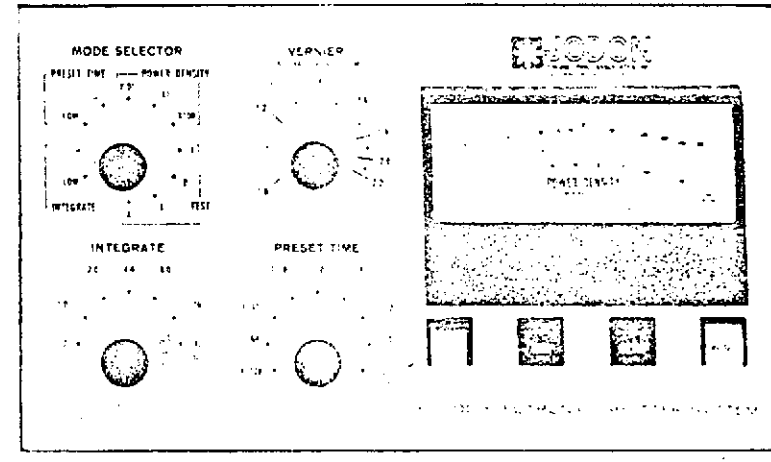

ACOUSTIC EMISSION TECHNIQUE

*EQUIPMENT

Dunegan Research Corp.
702 Audio Monitor 902 Flaw Locator
301 Totalizer 604 Monitor
502 Ramp Generator
402 Reset Clock
801P Preamplifier
D140A Differential Transducer
Hewlett Packard
7035B XY Recorder
Enerpac 10K Max
Hydrostatic Pump

INSTRUMENT

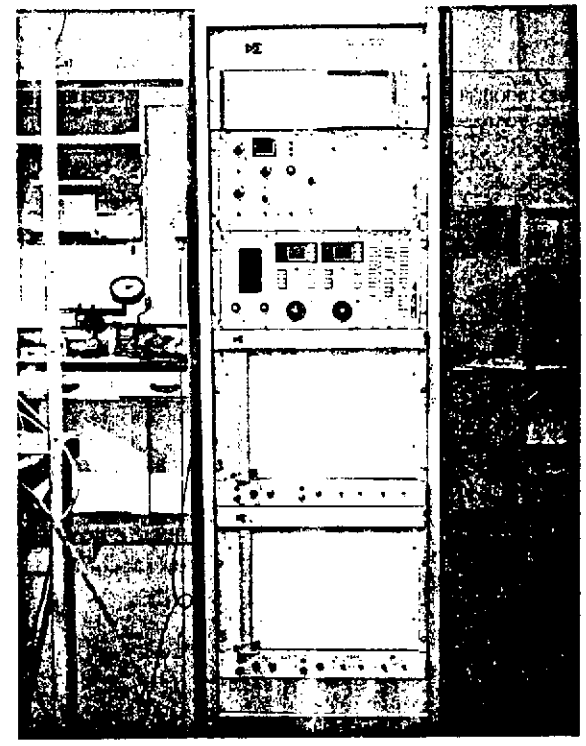

TEST CRITERIA

Mode: Sum [X] Log [ ]
Set: Rate [ ] Mem [X] Rate [ ]
Trans. Dual End
Sum X 10 Gain 80 DB*
Filter .1-HP * Reset Sec.
Ramp Gen. 10 Min.
Stress Hydrostatic

Total Count Recorded in 500 psi Increments
from 0 to 3500 psi

TEST LAY-OUT

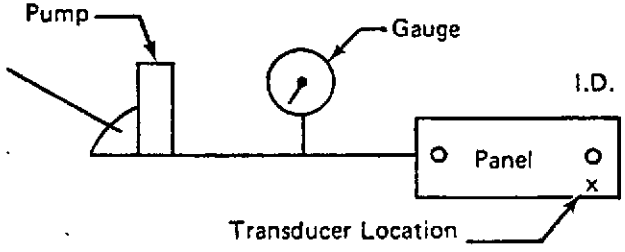

* 90 DB and No Filters for Copper-Copper

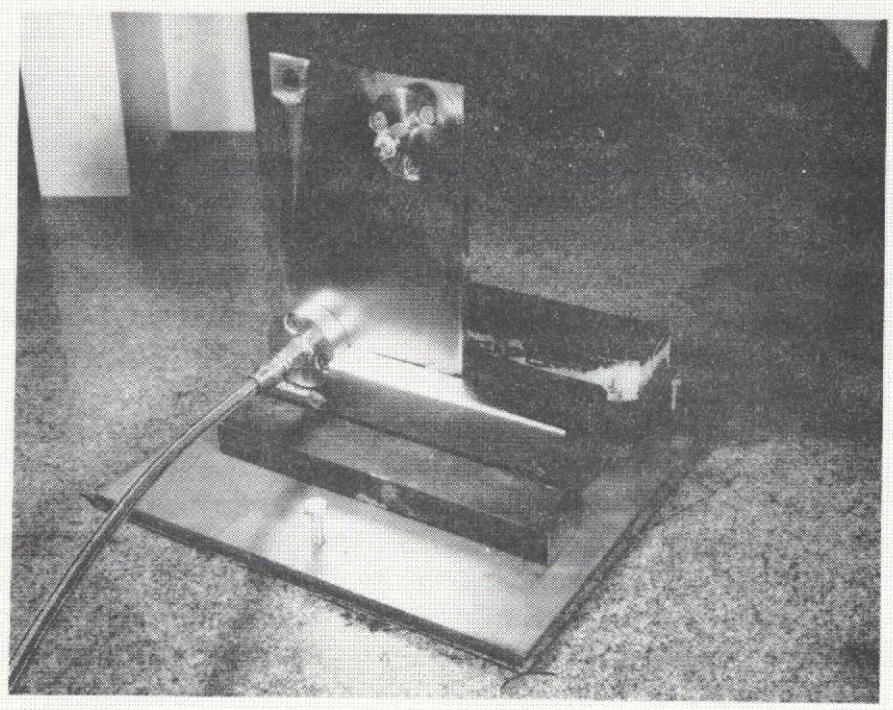

Figure 30. Holding Fixture and Test Panel for Holographic Evaluation

VII. TASK V - DESTRUCTIVE TESTING, METALLOGRAPHIC INSPECTION AND ANALYSIS

The panels evaluated for the NDE equipment limitations study in Task IV were hydrostatically tested to failure, and the bond or panel failure pressure was recorded for bond strength determination. During destructive testing, the progress of bond destruction was monitored with acoustic emission. At failure, the total emission count was recorded and reported on individual panels. This data appears on the NDE data pages of Appendix Section C.

Failure was achieved when evidence of external leakage, permanent deformation of the panel through bond failure, or yielding of the weakest portion of the coverplate or baseplate was achieved. Brazed panels were an exception. The stainless steel coverplates and OFHC copper baseplate were poor acoustic emittors. The braze was found to be a good emittor. These panels were pressurized beyond material yielding until acoustic counts from braze failure were obtained. This was done to obtain information in metallurgical sections which would indicate the mode of bond failure.

A. CALCULATED BOND STRENGTHS

Bond strengths were calculated from the pressures required to fail the test panel bonds. The failure load imposed on a land is the same as the combined hydrostatic pressure loading of the adjacent two channel passages. Excluding the manifolds, the area of a land is one-fourth the area of the two adjacent channels. The bond strength of the land bond is thus four times the channel pressure at failure.

The calculated bond strengths for all panels are shown in Tables XII, XIII, XIV and XV. In general, the bond strengths were as expected based on baseplate mechanical properties and the type of bond produced (i.e. - full, weak or nonbond). Braze panels

presented an exception in that all failures occurred in the braze alloy. Braze fillets or braze starved areas presented variable bond failure pressures on some panels.

On electroformed panels, unexpected failure pressures were obtained on a few panels due to the following reasons:

1. Tack bonding on the edges of planned, weak or non-bond defects.

2. Weaknesses induced on thin coverplate panels by machining damage.

3. Undetected porosity or laminations from repair efforts on porous areas where sufficient pickling to remove cold work could not be performed.

4. Unplanned weak bonds caused by solution drag-out in the preparation process for electroforming (this occurred only on a specific few copper coverplate panels).

These conditions were generally detected during nondestructive evaluation and confirmed by metallurgical analysis.

B. METALLOGRAPHIC INSPECTION AND ANALYSIS

Specimens for metallurgical analysis were cut from specific areas of the failed panels in Task IV to include an area of bond failure (where such occurred) and an unfailed region. Additional specimens were prepared from other areas of interest to determine reasons for unexpected NDE test results. Where possible, the samples were cut to provide a direction of viewing parallel to the planned bond defect. Sections transverse to the land edges were prepared on occasion to depict unusual edge effects which influenced NDE response.

Photomicrographs of the areas of interest are shown on the test panel fabrication data pages throughout Appendix Sections A and C. Generally, the pictures were taken at a magnification of 50 power. Where specific information was sought, the pictures were taken at other magnifications.

A special metallurgical evaluation of Panel C-08N (Appendix Figure C-22) was required because of an abnormal condition which was not planned and which affected interpretation of NDE results, Figure 31. This panel exhibited an abnormal acoustic emission count for a planned full bond and failure occurred at a lower pressure than expected. The photomicrograph reveals failure of the electroformed nickel coverplate adjacent to the center land and in a region of heavy porosity in the initial electrodeposit. A pinhole type leak occurred which was not detected until part way through the acoustic emission test.

This explains the abnormal acoustic count obtained and the lower than expected pressure required to fail the full bond.

C. CORRELATION OF NDE, DESTRUCTIVE TEST AND METALLURGICAL ANALYSIS RESULTS

Nondestructive test personnel were provided no prior knowledge of the planned defects or patterns used in the test panels for the NDE equipment limitations investigation (Task IV). NDE personnel evaluated the holography, ultrasonic and acoustic emission data and categorized each panel as to type and location of defects noted. The Program Technical Director evaluated the bond strength data, planned defect patterns and metallurgical analysis data to compare with the NDE categorizations. These evaluations are presented for each material combination in Tables XII, XIII, XIV and XV. The data as obtained are displayed on pages 70 through 193 in the Appendix.

In general, there was good correlation between the planned defects achieved and the results of the nondestructive evaluation. Most exceptions could be explained by unexpected or unplanned defects or conditions where were detected by the various NDE methods.

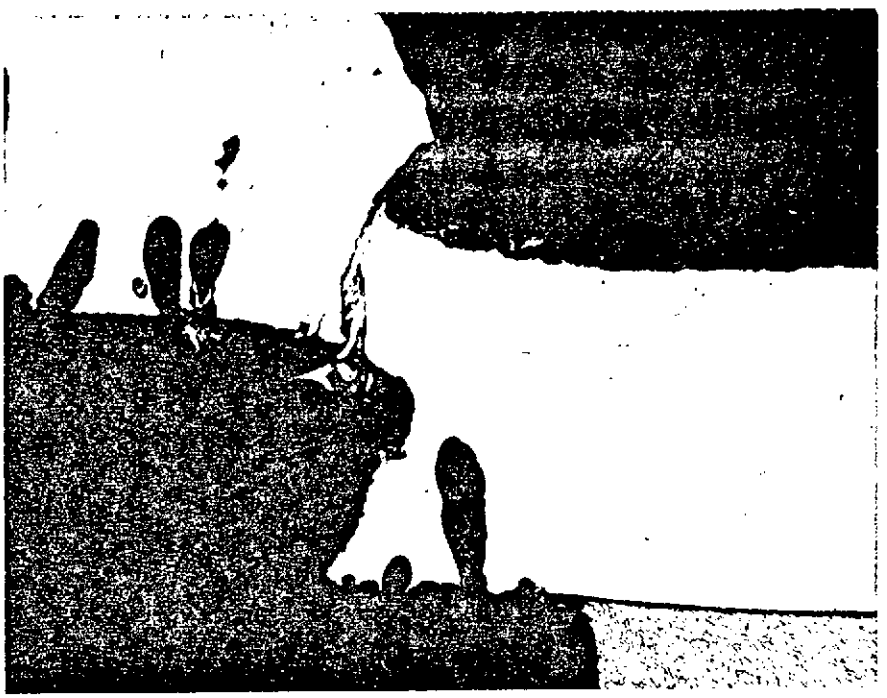

Figure 31. Metallurgical Section of Panel C-08N Showing Porous Region and Coverplate Failure Magnification 50X

TABLE XII - CORRELATION OF NDE RESULTS, BOND STRENGTHS AND METALLURGICAL RESULTS - EF NICKEL COVERPLATES ON NICKEL 200 BASEPLATES

PANEL NO.	PLANNED DEFECT	BOND INTEGRITY BASED ON NDE RESULTS	CALCULATED BOND STRENGTH	BOND INTEGRITY BASED ON METALLURGICAL ANALYSIS
N-11 "A" (See note below)	Full Bond	Weak bond based on high count from acoustic emission at low pressure. Holography indicates some weakness on center land edges.	276 MN/m^2 (40.0 kpsi)	Micros show some failure on extreme edges of lands with almost no metal disturbance. A weak edge bond existed.
N-29	Weak Bond Std. Flaw Area	Weak bond based on high count from AE at 19.3 MN/m^2 (2.8 kpsi). Hologram after AE indicated weak bond was converted to a partial nonbond.	276 MN/m^2 (40.0 kpsi)	Micros show weak bond separation with slight metal disturbance.
N-30	Weak Bond Std. Flaw Area	Holography indicated either a weak or nonbond on left side of center land. AE showed a high count typical of a weak bond. Weak bond judged to be $\frac{1}{2}$ land width by 12.70 mm. (0.50 in.) long.	276 MN/m^2 (40.0 kpsi)	Micros indicate a weak bond failure with slight metal disturbance.
N-38	Nonbond Std. Flaw Area	AE indicated very weak bonding which separated at low pressure. Holcgram confirmed separation after AE test. Most AE count came from the defect area.	157 MN/m^2 (22.8 kpsi)	Evidence of slight metal disturbance indicates some edge bonding may have occurred.
N-31	Weak Bond 2nd Flaw Area	Judged to be a full bond or strong weak bond. AE count was low, indicating a full bond. Holcgram after AE indicated some weakness about 1/3rd down from top of the center land.	235 MN/m^2 (34.0 kpsi)	Tack bonding possibly prevented failure of the planned weak bond at lower pressure. Weak bond was stronger than planned.

Note: All panel numbers with an "A" suffix were refabricated using the original baseplate.

TABLE XII - CORRELATION OF NDE RESULTS, BOND STRENGTHS AND METALLURGICAL RESULTS - EF NICKEL COVERPLATES ON NICKEL 200 BASEPLATES (CONTINUED)

PANEL NO.	PLANNED DEFECT	BOND INTEGRITY BASED ON NDE RESULTS	CALCULATED BOND STRENGTH	BOND INTEGRITY BASED ON METALLURGICAL ANALYSIS
N-32	Weak Bond 2nd Flaw Area	Strong weak bond as indicated by holography after AE. AE showed a low count which indicated a strong bond. The weakness from the hologram appeared in an area about 25.40 mm. (1.0 in.) long.	276 MN/m^2 (40.0 kpsi)	Micros indicated few, if any, signs of bond failure. Tack bonding over edge of land may have prevented failure in the planned weak bond.
N-39	Nonbond 2nd Flaw Area	Ultrasonic "C" scan and the hologram indicate a nonbond, length about 12.70 mm. (0.50 in.) long. High AE count from the defect area indicates some tack bonding.	66 MN/m^2 (9.6 kpsi)	Micro reveals separation of nonbond with signs of land edge metal disturbance indicating some edge bonding.
N-09 "A"	Full Bond Coverplate Thickness Thinner	Hologram indicates some weakness in center land about 2/3rds down from top of land. High AE count indicates a weak bond.	212 MN/m^2 (30.8 kpsi)	Micro reveals failure as occurring in the coverplate. Coverplate damage in machining required repair; plating restart was weak over repair area.
N-33	Weak Bond Coverplate Thickness Thinner	Weak bond. Ultrasonic "C" scan indicates some nonbond. AE shows a high count originating in a specific area. Hologram indicates a weakness in the same region.	185 MN/m^2 (26.8 kpsi)	Micro disclosed some failure in the planned weak bond area.
N-34 "A"	Weak Bond Coverplate Thickness Thinner	Weak bond. AE count was high at very low pressures. Ultrasonic "C" scan shows a small nonbond corresponding with weak bond indications from hologram.	97 MN/m^2 (14.0 kpsi)	Micro showed bond separation with little metal disturbance, indicating a very weak bond.

TABLE XII - CORRELATION OF NDE RESULTS, BOND STRENGTHS AND METALLURGICAL RESULTS - EF NICKEL COVERPLATES ON NICKEL 200 BASEPLATES

(CONTINUED)

PANEL NO.	PLANNED DEFECT	BOND INTEGRITY BASED ON NDE RESULTS	CALCULATED BOND STRENGTH	BOND INTEGRITY BASED ON METALLURGICAL ANALYSIS
N-40 "A"	Nonbond Coverplate Thickness Thinner	Nonbond as revealed from the ultrasonic "C" scan. The hologram shows a defect at the same location and indicates edge bonding of the nonbond at the left edge. This would account for some of the high AE count.	97 MN/m^2 (14.0 kpsi)	The micro shows a clear nonbond separation with no significant metal disturbance.
N-21	Full Bond Coverplate Strength Decreased	All NDE results indicated a full bond to be present.	221 MN/m^2 (32.0 kpsi)	Micro indicated a full bond with a small amount of land edge failure with some metal disturbance.
N-36	Weak Bond Coverplate Strength Decreased	Weak bond as indicated by AE high count at 13.8 MN/m^2 (2 kpsi). Hologram shows a trace of disturbance in the upper part of the center land after AE.	110 MN/m^2 (16 kpsi)	Micro shows weak bond separation with metal disturbance.
N-37	Weak Bond Coverplate Strength Decreased	Weak bond as indicated by the high AE count at very low pressures. The ultrasonic "C" scan indicates nonbond, but the hologram indicates some bonding was still present after the AE test, and the flaw locator shows count from the defect area.	88 MN/m^2 (12.8 kpsi)	Micro shows weak bond failure with significant metal disturbance.
N-41 "A"	Nonbond Coverplate Strength Decreased	The ultrasonic "C" scan and hologram indicate a nonbond, with some edge bonding present. Edge bonding was indicated by high AE count at low pressure.	64 MN/m^2 (9.2 kpsi)	Metallurgical section showed nonbond separation with little metal disturbance.

TABLE XII - CORRELATION OF NDE RESULTS, BOND STRENGTHS AND METALLURGICAL RESULTS - EF NICKEL COVERPLATES ON NICKEL 200 BASEPLATES (CONTINUED)

PANEL NO.	PLANNED DEFECT	BOND INTEGRITY BASED ON NDE RESULTS	CAICULATED BOND STRENGTH	BOND INTEGRITY BASED ON METALLURGICAL ANALYSIS
N-13	Full Bond Surface Flatness	Full bond based on low count from AE. Hologram showed the effect of surface flatness but no sign of a defect.	204 MN/m^2 (29.6 kpsi)	Metallurgical section revealed no bond failure.
N-46	Weak Bond Surface Flatness	Extremely weak bond based on the high AE count at low pressure and the hologram. Ultrasonic "C" scan indicates a nonbond; it may not have the sensitivity to detect the intermittent weak bonding.	235 MN/m^2 (34.0 kpsi)	Micro showed bond failure with little metal disturbance between the initial nickel flash and the final coverplate build-up, indicating a very weak bond.
N-42	Nonbond Surface Flatness	Nonbond as indicated by all three NDE tests. The AE count and flaw locator indicated a possible trace of tack bond.	97 MN/m^2 (14.0 kpsi)	Micro showed nonbond separation with no sign of metal disturbance.
N-56	Full Bond Narrow Lands	Ultrasonic "C" scan and the hologram indicated a full bond. High AE count was due to a leak developed during test.	Special Panel Not Destructed	Not Sectioned.
N-57	Weak Bond Narrow Lands	Ultrasonics and holography indicated a nonbond. AE count was typical of a nonbond.	Special Panel Not Destructed	Not Sectioned.
N-58	Nonbond Narrow Lands	All NDE tests indicate a nonbond.	Special Panel Not Destructed	Not Sectioned.

TABLE XIII - CORRELATION OF NDE RESULTS, BOND STRENGTHS AND METALLURGICAL RESULTS - EF NICKEL COVERPLATES ON OFHC COPPER BASEPLATES

PANEL NO.	PLANNED DEFECT	BOND INTEGRITY BASED ON NDE RESULTS	CALCULATED BOND STRENGTH	BOND INTEGRITY BASED ON METALLURGICAL ANALYSIS
C-08N "A"	Full Bond	Ultrasonic "C" scan and hologram indicated a full bond, or strong weak bond. High AE count indicated bond was weak.	185 MN/m^2 (26.8 kpsi)	Micro showed heavy base metal disturbance when failure occurred. The coverplate failed in the EF nickel due to a porous first layer.
C-28N	Weak Bond Std. Flaw Area	Full bond based on low AE count	207 MN/m^2 (30.0 kpsi)	Micro showed initiation of bond failure. Based on this and most count on flaw locator being from the planned flaw region, the defect was a "strong" weak bond.
C-29N	Weak Bond Std. Flaw Area	Nonbond based on ultrasonic "C" scan and hologram. Nonbond was $\frac{1}{2}$ land width. AE count was low for a weak bond.	220 MN/m^2 (32.0 kpsi)	Lack of base metal disturbance in micro indicates nonbond was present. AE flaw locator shows some tack bonding may have existed.
C-30N	Nonbond Std. Flaw Area	Nonbond based on all three NDE methods. AE count was low, indicating no weak bonding was present.	91 MN/m^2 (13.2 kpsi)	Micro indicated the planned nonbond was achieved. A trace of tack bonding is evident.
C-32N	Weak Bond 2nd Flaw Area	Weak bond based on hologram. Ultrasonic "C" scan shows some localized nonbond. AE results were not sufficiently informative.	110 MN/m^2 (16.0 kpsi)	Weak bond was confirmed by the micro. Base metal disturbance was noted.

TABLE XIII - CORRELATION OF NDE RESULTS, BOND STRENGTHS AND METALLURGICAL RESULTS - EF NICKEL COVERPLATES ON OFHC COPPER BASEPLATES

(CONTINUED)

PANEL NO.	PLANNED DEFECT	BOND INTEGRITY BASED ON NDE RESULTS	CALCULATED BOND STRENGTH	BOND INTEGRITY BASED ON METALLURGICAL ANALYSIS
C-33N	Weak Bond 2nd Flaw Area	Nonbond based on ultrasonic "C" scan and hologram. Low AE count at low pressure indicates little, or no weak bond failure. Defect appears ½ land wide x 12.70 mm. (0.50 in.) long.	207 MN/m^2 (30.0 kpsi)	Metallurgical sections show defect to be ½ land width and at least partly nonbonded as evidenced by a lack of metal disturbance.
C-34N	Nonbond 2nd Flaw Area	Weak bond based on ultrasonic "C" scan and low pressure AE count. Thin weak bond separated in holography testing.	124 MN/m^2 (18.0 kpsi)	Micro indicated some metal disturbance typical of very weak bonds.
C-09N	Full Bond Coverplate Thickness Thinner	Judged to be a weak bond as a result of the hologram. The AE results indicate a full bond.	138 MN/m^2 (20.0 kpsi)	Metallurgical evidence indicated a full bond was obtained. The hologram pressure may have been too high for the thin coverplate.
C-35N"A"	Weak Bond Coverplate Thickness Thinner	Weak bond based on high AE count at low pressures Ultrasonic "C" scan revealed trace of defect. Hologram pattern difficult to interpret due to thin coverplate.	97 $MN/m.^2$ (14.0 kpsi)	Micros confirmed weak bond defect separation and base metal disturbance.
C-36N"A"	Weak Bond Coverplate Thickness Thinner	Weak bond based on high AE count at low pressure. Most flaw locator count was about 1/3rd down from top of land. Hologram show disturbances possibly due to thin coverplate.	74 $MN/m.^2$ (10.8 kpsi)	Micros indicate a bond failure with little metal disturbance - possibly a very weak bond.

TABLE XIII - CORRELATION OF NDE RESULTS, BOND STRENGTHS AND METALLURGICAL RESULTS - EF NICKEL COVERPLATES ON OFHC COPPER BASEPLATES

(CONTINUED)

PANEL NO.	PLANNED DEFECT	BOND INTEGRITY BASED ON NDE RESULTS	CALCULATED BOND STRENGTH	BOND INTEGRITY BASED ON METALLURGICAL ANALYSIS
C-37N	Nonbond Coverplate Thickness Thinner	Nonbond based on ultrasonic "C" scan and hologram. AE curve indicates a nonbond also.	74 $MN/m.^2$ (10.8 kpsi)	Micro shows a nonbond separation with no metal disturbance.
C-06N	Full Bond Coverplate Strength Weaker	Full bond is indicated by all NDE methods.	276 $MN/m.^2$ (40.0 kpsi)	Metallurgical section shows a full bond to exist.
C-38N	Weak Bond Coverplate Strength Weaker	Judged to be a full bond. Hologram showed a small disturbance about 1/3rd down from top of center land, but nothing significant.	138 $MN/m.^2$ (20.0 kpsi)	Micro shows the planned weak bond separation with little metal disturbance. NDE portion of AE test was terminated at too low a pressure.
C-39N	Weak Bond Coverplate Strength Weaker	Judged to be a full bond based on AE count and hologram showing little distrubance.	221 $MN/m.^2$ (32.0 kpsi)	Micro shows weak bond failure. Bond was stronger that expected. Base metal disturbance was noted.
C-03N	Nonbond Coverplate Strength Weaker	Nonbond based on hologram and ultrasonic "C" scan. AE flaw locator indicated some tack bonding in nonbond.	94 $MN/m.^2$ (13.6 kpsi)	Micro confirmed nonbond defect had some tack bonding as noted from base metal disturbance.

TABLE XIV - CORRELATION OF NDE RESULTS, BOND STRENGTHS AND METALLURGICAL RESULTS - EF COPPER COVERPLATES ON OFHC COPPER BASEPLATES

PANEL NO.	PLANNED DEFECT	BOND INTEGRITY BASED ON NDE RESULTS	CALCULATED BOND STRENGTH	BOND INTEGRITY BASED ON METALLURGICAL ANALYSIS
C-01C	Full Bond	Full bond is indicated by all NDE methods.	221 $MN/m.^2$ (32.0 kpsi)	Micro indicated a full bond.
C-16C	Weak Bond Std. Flaw Area	Weak bond indicated from hologram and higher AE count than noted on Panel C-01C.	140 $MN/m.^2$ (20.4 kpsi)	Micro confirmed weak bond failure with heavy metal disturbance.
C-17C	Weak Bond Std. Flaw Area	Full bond indicated from AE count and hologram.	105 $MN/m.^2$ (15.2 kpsi)	Weak bond $\frac{1}{2}$ land wide was confirmed by micros.
C-18C "A"	Nonbond Std. Flaw Area	Weak bond as indicated by high AE count at low pressure.	52 $MN/m.^2$ (7.6 kpsi)	Planned nonbond did not fail. An unplanned weak bond did fail.
C-19C	Weak Bond 2nd Flaw Area	Weak bond indicated by high AE count at low pressure and a defect pattern on the hologram.	50 $MN/m.^2$ (7.2 kpsi)	Micro confirmed the planned weak bond failure.
C-20C	Weak Bond 2nd Flaw Area	Weak bond based on high AE count at low pressure. Hologram shows slight indication of edge defect on center land.	52 $MN/m.^2$ (7.6 kpsi)	Metallurgical section confirmed weak bond was $\frac{1}{2}$ land wide.
C-21C "A"	Nonbond 2nd Flaw Area	Nonbond based on AE count at low pressure. Hologram showed no specific defects.	72 $MN/m.^2$ (10.4 kpsi)	Micros showed no failure in planned nonbond area. Failure was in an unplanned weak bond - the dominant flaw.

TABLE XIV - CORRELATION OF NDE RESULTS, BOND STRENGTHS AND METALLURGICAL RESULTS - EF COPPER COVERPLATES ON OFHC COPPER BASEPLATES

(CONTINUED)

PANEL NO.	PLANNED DEFECT	BOND INTEGRITY BASED ON NDE RESULTS	CALCULATED BOND STRENGTH	BOND INTEGRITY BASED ON METALLURGICAL ANALYSIS
C-04C	Full Bond Coverplate Thickness Thinner	Full bond based on low AE count. Hologram showed disturbances which may have been due to the thin coverplate.	97 $MN/m.^2$ (14.0 kpsi)	Micro confirmed full bond to be present.
C-22C "A"	Weak Bond Coverplate Thickness Thinner	Weak bond indicated by high AE count at low pressure. Hologram showed no significant defect pattern.	39 $MN/m.^2$ (5.6 kpsi)	Weak bond failure was confirmed by metallurgical analysis. Metal disturbance noted.
C-23C "A"	Weak Bond Coverplate Thickness Thinner	Weak bond based on high AE count at low pressure. All count was in a specific area on the flaw locator.	64 $MN/m.^2$ (9.2 kpsi)	Planned defect showed no failure due to rupture of the thin coverplate.
C-24C "A"	Nonbond Coverplate Thickness Thinner	Nonbond indicated by ultrasonics "C" scan and hologram. AE indicated weakness on lower end of panel.	30 $MN/m.^2$ (4.4 kpsi)	Micro showed planned nonbond separation.
C-12C "A"	Full Bond Coverplate Strength Decreased	"Strong" weak bond indicated by AE count. No defects noted on hologram.	152 $MN/m.^2$ (22 kpsi)	Micro disclosed a weak bond at the lower end of 1st and 2nd land.
C-25C "A"	Weak Bond Coverplate Strength Decreased	Full bond based on hologram and low AE count.	157 $MN/m.^2$ (22.8 kpsi)	Micros disclosed planned weak bond was a full bond. Failure occurred in coverplate.

TABLE XIV - CORRELATION OF NDE RESULTS, BOND STRENGHTS AND METALLURGICAL RESULTS - EF COPPER COVERPLATES ON OFHC COPPER BASEPLATES

(CONTINUED)

PANEL NO.	PLANNED DEFECT	BOND INTEGRITY BASED ON NDE RESULTS	CALCULATED BOND STRENGTH	BOND INTEGRITY BASED ON METALLURGICAL ANALYSIS
C-26C "A"	Weak Bond Coverplate Strength Decreased	Weak bond indicated by high AE count.	207 $MN/m.^2$ (30.0 kpsi)	Planned weak bond did not fail. Failure occurred on full bond on 3rd land. AE noise was from failing burrs from machining the baseplate.
C-27C	Nonbond Coverplate Strength Decreased	Weak bond based on high AE count at low pressure.	44 $MN/m.^2$ (6.4 kpsi)	Micros disclosed weak bonding in the planned nonbond. Very weak bond detected on Land 3.

TABLE XV - CORRELATION OF NDE RESULTS, BOND STRENGTHS AND METALLURGICAL RESULTS - STAINLESS STEEL COVERPLATES BRAZED TO OFHC COPPER BASEPLATES

PANEL NO.	PLANNED DEFECT	BOND INTEGRITY BASED ON NDE RESULTS	CALCULATED BOND STRENGTH	BOND INTEGRITY BASED ON METALLURGICAL ANALYSIS
B-04	Full Bond	Full bond indicated by low AE count and no hologram disturbances.	149 $MN/m.^2$ (21.6 kpsi)	Micros confirmed full bond was achieved.
B-18	Weak Bond Std. Flaw Area	Small nonbonds were noted in "C" scan and defects found in the hologram.	111 $MN/m.^2$ (16.8 kpsi)	Micros confirmed planned braze voids to produce "weak" bond.
B-16	Weak Bond Std. Flaw Area	Flaws composed of small nonbonds noted in "C" scan. Hologram also indicates defects.	113 $MN/m.^2$ (16.4 kpsi)	Micros verified planned braze voids to produce "weak" bond.
B-08	Nonbond Std. Flaw Area	Hologram and "C" scan indicate nonbond 1/3rd down from top of center land.	138 $MN/m.^2$ (20.0 kpsi)	Micros verified planned nonbond.
B-20	Weak Bond 2nd Flaw Area	Hologram disclosed a flaw in center land. "C" scan showed same flaw to be thin nonbonds.	130 $MN/m.^2$ (18.8 kpsi)	Micros confirmed planned braze voids to produce "weak" bond.
B-17	Weak Bond 2nd Flaw Area	Low pressure AE count indicated weak bonding. Flaw pattern noted in "C" scan and holography on center land.	113 $MN/m.^2$ (16.4 kpsi)	Micros disclosed planned braze voids to produce "weak" bond.
B-09	Nonbond 2nd Flaw Area	Nonbond based on large defect detected by "C" scan and hologram.	135 $MN/m.^2$ (19.6 kpsi)	Metallurgical section revealed planned nonbond as void of braze.
B-06	Full Bond Coverplate Thickness Thicker	Full bond as indicated by "C" scan and holo-	204 $MN/m.^2$ (29.6 kpsi)	Micros confirmed the planned full bond.

TABLE XV - CORRELATION OF NDE RESULTS, BOND STRENGTHS AND METALLURGICAL RESULTS - STAINLESS STEEL COVERPLATES BRAZED TO OFHC COPPER BASEPLATES

(CONTINUED)

PANEL NO.	PLANNED DEFECT	BOND INTEGRITY BASED ON NDE RESULTS	CALCULATED BOND STRENGTH	BOND INTEGRITY BASED ON METALLURGICAL ANALYSIS
B-19	Weak Bond Coverplate Thickness Thicker	Small uniform nonbond flaws on center land. "C" scan shows gross nonbond on right side of panel.	Not Destructed	Not sectioned due to unplanned braze nonbond.
B-15	Weak Bond Coverplate Thickness Thicker	Nonbond indicated by "C" scan and by holography in center land.	166 $MN/m.^2$ (24.0 kpsi)	Micros indicated planned weak bond was a nonbond.
B-11	Nonbond Coverplate Thickness Thicker	Nonbond based on the large void noted in the "C" scan and hologram.	193 $MN/m.^2$ (28.0 kpsi)	Micros confirmed the planned nonbond.

D. TEST CYLINDER RESULTS

The holographic results for the three test sections of the cylinder are shown in Figure 32. The planned weak bond in Section 2 of the cylinder was sufficiently weak that the bond failed and reverted to a nonbond at 3.1 $MN/m.^2$ (450 psi) pressure. The planned nonbond in Section 3 showed indications of a partial bonding, since the hologram bands do not cross the land.

The acoustic emission results were difficult to interpret due to the fact that the transducers were repositioned from Section 2 to Section 3 to acquire more precise flaw locator data. Consequently, no emission curves were plotted. The acoustic emission counting system was placed on "hold" during relocation of the transducers. The flaw locator responses are shown in Figure 33. The high emission indicated at the lower end of the land in the flaw locator picture for Section 3 confirms the partial bonding detected by holography in the same area.

TEST CYLINDER HOLOGRAPHIC RESULTS

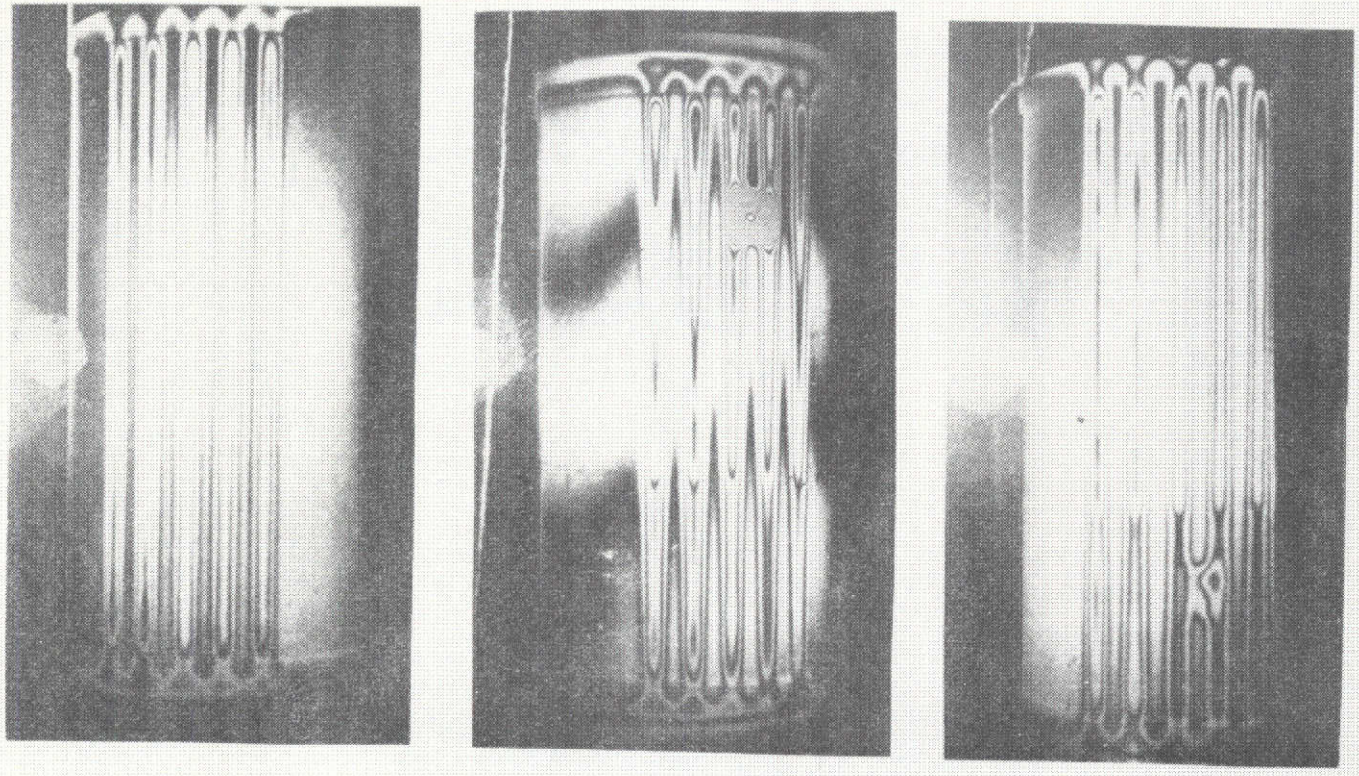

PLANNED
FULL BOND

SECTION 1

PRESSURE:
$1.38 \times 10^6 N/M^2$
(200 PSI)

PLANNED WEAK BOND
(ACTUALLY NONBOND)

SECTION 2

PRESSURE:
$3.10 \times 10^6 N/M^2$
(450 PSI)

PLANNED
NONBOND
(SHOWS SOME BOND)
SECTION 3

PRESSURE:
$1.725 \times 10^6 N/M^2$
(250 PSI)

Figure 32. Holograms of the Various Test Sections of the Cylinder

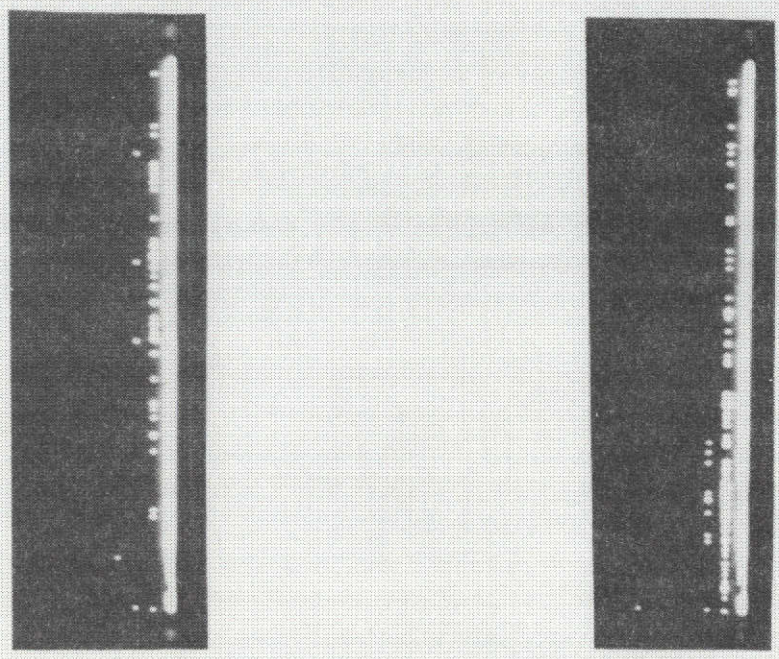

Section 2
(Weak Bond)

Section 3
(Nonbond)

Figure 33. Flaw Locator Responses for the Test Cylinder

VIII - CONCLUSIONS AND RECOMMENDATIONS

Results of this investigation show that all three NDE tests are required to fully interrogate regeneratively cooled thrust chambers. The equipment limitations and capabilities are discussed below by NDE test method. Page numbers referenced in the following discussion are those of the appendix volume of this report.

A. ULTRASONIC "C" SCAN

Ultrasonic "C" scan performed as expected in that only nonbond defects were detected. It afforded an initial screening method to detect large unplanned nonbonds which would have made further testing uneconomical and of no technical value (Panel B-19, page 189). The significant advantage of this method over holography is the size of nonbond readily detectable (Panel B-16, page 177).

Providing the planned bond defect was a nonbond, or contained areas of nonbond, ultrasonic "C" scan was generally able to detect the flaw. This NDE method was not affected by defect area or coverplate strength for the ranges of these variables investigated.

Variation of coverplate thickness was found to affect the sensitivity of ultrasonic flaw detection, but this effect appeared to be influenced by the combination of materials evaluated. The combination of electroformed nickel bonded to nickel presented the greatest nonbond detection difficulties. Panel N-38, page 77, appears to have a full bond in the actual nonbond area. Panel N-40 "A", page 91, appears to contain the planned nonbond, but the hologram shows unplanned bonding on the left side of the middle land. For the material combination of electroformed nickel on copper, ultrasonics defined the nonbonds, and showed regions of intimate contact or possible "tack" bond within the planned flaw (Panel C-34N, page 125 and Panel C-37N, page 133). Similar sensitivity was noted on the dissimilar metal combination used in the brazed panels and on the electroformed copper on OFHC copper combination.

Coverplate flatness did not deter ultrasonic "C" scan from detecting nonbonds (Panel N-42, page 105), but a weak bond falsely appeared as a nonbond (Panel N-46, page 103).

Ultrasonic "C" scan could not be successfully applied to the cylindrical test hardware due to the curved surface of the test specimen. Testing would require expensive special tooling which was beyond the scope of this investigation.

B. ACOUSTIC EMISSION

The acoustic emission test with the supporting flaw locator system provided excellent capability to detect and locate (with respect to a single planar coordinate) planned weak bonds in the equipment limitation investigation. It also detected and located defects other than those planned. In particular, this technique disclosed nonbonds and unexpected weak bonds existing on panels with electroformed copper coverplates. As a result, it was possible to determine the processing variable which caused these weak regions and correct the fabrication operation. Examples of unplanned weak bonds detected are illustrated in data for Panel C-21C "A", page 155; Panel C-12C "A", page 165; and Panel C-27C, page 170.

Because of uncontrollable variables in the fabrication process, acoustic emission count could not be directly correlated with quantitative bond strength values. It did provide an excellent means of detecting impending failure of bonds or coverplate by monitoring count summation change in the recording mode.

The sensitivity of acoutic emission as an NDE method is directly affected by the test specimen materials of construction. Copper and certain stainless steels are low acoustic emittors. Nickel and the silver base braze alloy used in this program were good acoustic emittors. As a result, it was necessary to adjust equipment sensitivity to obtain interpretable results without risking destruction of the test panels.

On the brazed panels, bond failure occurred in the braze alloy, regardless of defect size or coverplate thickness. Coverplate buckling usually occurred prior to braze failure initiation. Consequently, the panel would be deformed before acoustic emissions were recorded. The result was that acoustic emission data indicated no distinguishing patterns for the various bond integrities investigated. Fortunately, the planned bond defects were easily detected by the other two NDE methods without application of high test pressure.

On electroformed coverplate panels, the most significant unplanned variables in panel fabrication which interferred with acoustic emission bond strength evaluation were land bcnd edge effects (Panel N-31, page 79) and undetected porosity near the bond interface (Panel N-56, page 107). This problem has a potential solution in that the effect of these processing variables can be more accurately assessed by stopping the acoustic emission test when unusual indications warrant and applying the holography test again to determine if bond region degradation has occurred.

In general, weak bond geometry did not interfere with acoustic emission sensitivity as long as the defect edge length exposed to pressure remained the same (Panel N-29, page 73 and Panel N-30, page 75). Doubling the area of weak bond did not produce a corresponding increase in emission summation for a given pressure. This may be due to acoustic emissions originating in the weakest bond portion of the defect - regardless of size. True size of the flaw may not be detectable with acoustic emission alone without risking failure of the test specimen.

Weak bonds usually were characterized by acoustic emission summation - pressure curves of steep slope. Exceptions to this general rule were noted when the "weak" bond strength was high, such as experienced on Panel N-31, page 79, and Panel C-39N, page 139.

The corresponding curves for full bonds had low angle slopes, except for cases where anomalies existed such as porosity, laminations or unusual edge effects.

L-2

True nonbonds resulted in acoustic emission - pressure curves of slope steeper than full bonds, but shallower than weak bonds. Frequently the nonbonds contained localized weak bonds which resulted in hybrid acoustic emission plots between those of weak and nonbonds.

Decreasing coverplate thickness or yield strength did not deter the capability of acoustic emission to provide interpretable data. These changes generally decreased the pressures at which meaningful acoustic emission responses occurred. Bond quality was still distinguishable by acoustic emission when the surface flatness was varied. This variable influenced the emission count summations, due to cover buckling strength variations, but the ensuing effect on the curves characteristic of each bond type were not seriously affected.

This NDE method proved readily adaptable to the test cylinder configuration and the planned defects were roughly located with a two transducer flaw locator system. A more complex flaw locator system would be required to define the exact lands on which the flaws existed.

C. HOLOGRAPHY

The sensitivity of holography was found to be related to coverplate buckling strength - a factor used to design coverplate thickness for optimum NDE response. This is illustrated by comparing holographic results for Panels N-25, page 45, and Panel N-26, page 47. Excessive coverplate thickness requires higher pressures than desired to cause a coverplate stress reaction at the defect in order to be detected by holography. By optimizing the maximum coverplate thickness investigated in this study, lower pressures could be used for interpretable holograms. This minimized data loss from the Kaiser effect in subsequent acoustic emission studies.

The holography response for large nonbonds appears on the hologram as bands crossing the bonding land. Small nonbonds and large weak bonds are indicated by band disturbances in the adjacent channel areas.

Holography demonstrated an ability to detect all nonbonds identified by ultrasonic "C" scan, regardless of coverplate thickness, flaw area, or coverplate strength. It provided a more complete analysis of nonbonds than ultrasonic "C" scans in that localized "tack bonding was defined. NDE test results for Panel N-40 "A", page 91; Panel N-41 "A", page 99; and Panel C-33N, page 123 illustrate this advantage of holography over ultrasonics.

Holography was less reliable in detecting weak bonds. The ability of this test to detect such defects appeared dependent on relative strength of the weak bond, length of weak bond edge exposure to the pressurizing channel, and thickness of the coverplate. Panel N-30, page 75, contained a weak bond with exposed edge twice as long as that on Panel N-29, page 73. The Panel N-30 weak bond was readily detected by holography prior to exposure to the higher pressures used in acoustic emission. The "shorter" weak bond on Panel N-29 was not readily discerned at low holographic test pressures.

Proper sequencing of holographic evaluation can overcome most of the limitations imposed by coverplate variables. When Panel N-29 was evaluated by acoustic emission, an indication of a bond defect was noted at a moderate pressure. By re-examining the panel with low pressure holography, the defect was accurately identified by size and location.

Moderate variation of coverplate flatness did not impair holographic detection of the various bond integrities.

Holography proved to be one of the best methods for detecting defects in brazed panels where both primary bonded plates were poor acoustic emittors.

The achievement of successful holograms on the cylindrical test specimen represents a major advancement in developing holography from a laboratory test to a useful production evaluation technique. This represented a successful transition of holography from a flat panel to a three dimensional surface of investigation without loss of sensitivity.

D. RECOMMENDATIONS

It is recommended that further work be performed with these nondestructive techniques to complete the transition from test panels to larger complex configurations used in aerospace applications.

It is suggested that additional work be performed to evaluate the effect of secondary fabrication operations on NDE response.

Since actual production hardware is usually designed with a strength safety factor, resulting structural thicknesses and resistance to pressure stresses can be expected to differ from those encountered in this work. Such structures should be examined to determine which, if any, NDE technique modifications should be used. By example, the acoustic emission equipment sensitivity can be changed for good or poor emittors and for thick or thin stressed members of a structure.

In addition, consideration of the point in fabrication time or sequence to apply selected NDE tests should be evaluated by the nondestructive evaluation personnel working with the design engineer and manufacturing personnel.

Efforts to date have examined the simulated chamber wall structures from the outer shell side. Actual thrust chambers often have pressure fittings, manifolds, and miscellaneous attached equipment which would interfere with this mode of examination. Work should be initiated to nondestructively examine these structures from the inside (liner) surface. This will probably require development of special tooling for some of the NDE techniques.

DISTRIBUTION LIST FOR FINAL REPORT

NAS3-10[illegible]

NASA CR-134656
and CR-134657

REPORT COPIES R	D	RECIPIENT	DESIGNEE
		National Aeronautics & Space Administration Lewis Research Center 21000 Brookpark Road Cleveland, Ohio 44135	
1		Attn: Contracting Officer, MS 500-313	
5		E. A. Bourke, MS 500-205	
1		Technical Report Control Office, MS 5-5	
1		Technology Utilization Office, MS 3-16	
2		AFSC Liaison Office, 501-3	
2		Library	
1		Office of Reliability & Quality Assurance, MS 500-211	
1		J. W. Gregory Chief, MS 500-203	
16		R. A. Duscha Project Manager, MS 500-203	
1		Alex Vary, MS 106-1	
1		R. F. Lark, MS 49-1	
1		W. E. Russell, MS 14-1	
1		S. J. Klima, MS 106-1	
1		Director, Shuttle Technology Office, RS Office of Aeronautics & Space Technology NASA Headquarters Washington, D.C. 20546	
2		Director, Space Propulsion & Power, RP Office of Aeronautics & Space Technology NASA Headquarters Washington, D.C. 20546	
1		Director, Launch Vehicles & Propulsion, SV Office of Space Science NASA Headquarters Washington, D.C. 20546	
1		Director, Materials & Structures Division, RW Office of Aeronautics & Space Technology NASA Headquarters Washington, D.C. 20546	
1		Director, Advanced Manned Missions, MT Office of Manned Space Flight NASA Headquarters Washington, D.C. 20546	

REPORT COPIES R	D	RECIPIENT	DESIGNEE
20		**National Technical Information Service** **Springfield, Virginia 22151**	
1		**National Aeronautics & Space Administration** **Ames Research Center** **Moffett Field, California 94035** **Attn. Library**	**Hans M. Mark** **Mission Analysis Division**
1		**National Aeronautics & Space Administration** **Flight Research Center** **P.O. Box 273** **Edwards, California 93523** **Attn: Library**	
1		**Director, Technology Utilization Division** **Office of Technology Utilization** **NASA Headquarters** **Washington, D.C. 20546**	
1		**Office of the Director of Defense** **Research & Engineering** **Washington, D.C. 20301** **Attn: Office of Asst. Dir. (Chem. Technology)**	
2		**NASA Scientific & Technical Information Facility** **P.O. Box 33** **College Park, Maryland 20740** **Attn: NASA Representative**	
1		**National Aeronautics & Space Administration** **Goddard Space Flight Center** **Greenbelt, Maryland 20771** **Attn: Library**	**Merland L. Moseson, Code 620**
1		**National Aeronautics & Space Administration** **John F. Kennedy Space Center** **Kennedy Space Center, Florida 32899** **Attn: Library**	**Dr. Kurt H. Debus**
1		National Aeronautics & Space Administration Langley Research Center	E. Cortwright, Director
	1	Langley Station	Lewis Thurston, Jr.
	1	Hampton, Virginia 23665	E. Hoffman
		Attn: Library	

REPORT COPIES R	REPORT COPIES D	RECIPIENT	DESIGNEE
1	1	National Aeronautics & Space Administration Lyndon B. Johnson Space Center Houston, Texas 77058	J. G. Thibodaux, Jr. Chief, Propulsion & Power Division
	1	Attn: Library	W. L. Castner
1		National Aeronautics & Space Administration	Hans G. Paul
	1	George C. Marshall Space Flight Center	Jerry Thomson
	1	Marshall Space Flight Center, Alabama 35812 Attn: Library	Dr. Ray Gause
1		Jet Propulsion Laboratory 4800 Oak Grove Drive Pasadena, California 91103 Attn: Library	Henry Burlage, Jr. Duane Dipprey
1		Defense Documentation Center Cameron Station Building 5 5010 Duke Street Alexandria, Virginia 22314 Attn: TISIA	
1		RTD (RTMP) Bolling Air Force Base Washington, D.C. 20332	
1		Arnold Engineering Development Center Air Force Systems Command Tullahoma, Tennessee 37389 Attn: Library	Dr. H. K. Doetsch
1		Advanced Research Projects Agency Washington, D.C. 20525 Attn: Library	
1	1	Aeronautical Systems Division Air Force Systems Command Wright-Patterson Air Force Base Dayton, Ohio 45433 Attn: Library	D. L. Schmidt Code ARSCNC-2
1		Air Force Missile Test Center Patrick Air Force Base, Florida Attn: Library	L. J. Ullian

REPORT COPIES R	D	RECIPIENT	DESIGNEE
1		Air Force Systems Command Andrews Air Force Base Washington, D.C. 20332 Attn: Library	Capt. S. W. Bowen SCLT
1	1	Air Force Rocket Propulsion Laboratory (RPR) Edwards, California 93523 Attn: Library	Donald Penn Robert Wiswell
1		Air Force Rocket Propulsion Laboratory (RPM) Edwards, California 93523 Attn: Library	
1		Air Force FTC (FTAT-2) Edwards Air Force Base, California 93523 Attn: Library	Donald Ross
1		Air Force Office of Scientific Research Washington, D.C. 20333 Attn: Library	SREP, Dr. J. F. Masi
1		Space & Missile Systems Organization Air Force Unit Post Office Los Angeles, California 90045 Attn: Technical Data Center	
1		Office of Research Analyses (QAR) Holloman Air Force Base, New Mexico 88330 Attn: Library RRRD	
1		U.S. Air Force Washington, D.C. Attn: Library	Col. C. K. Stambaugh, Code AFRST
1		Commanding Officer U.S. Army Research Office (Durham) Box CM, Duke Station Durham, North Carolina 27706 Attn: Library	
1		U.S. Army Missile Command Redstone Scientific Information Center Redstone Arsenal, Alabama 35808 Attn: Document Section	Dr. W. Wharton

REPORT COPIES R	D	RECIPIENT	DESIGNEE
1		Bureau of Naval Weapons Department of the Navy Washington, D.C. Attn: Library	J. Kay, Code RTMS-41
1		Commander U.S. Naval Missile Center Point Mugu, California 93041 Attn: Technical Library	
1		Commander U. S. Naval Weapons Center China Lake, California 93557 Attn: Library	
1		Commanding Officer Naval Research Branch Office 1030 E. Green Street Pasadena, California 91101 Attn: Library	
1		Director (Code 6180) U.S. Naval Research Laboratory Washington, D.C. 20390 Attn: Library	H. W. Carhart J. M. Krafft
1		Picatinny Arsenal Dover, New Jersey 07801 Attn: Library	I. Forsten
1		Air Force Aero Propulsion Laboratory	R. Quigley
	1	Air Force Systems Command U. S. Air Force Wright-Patterson AFB, Ohio 45433 Attn: APRP (Library)	Tom Cooper
1		Acoustic Emission Technology Corp. 1828A Tribute Road Sacramento, California 95815 Attn: Allen Green	
1	1	Aerojet Liquid Rocket Company	R. J. LaBotz
	1	P.O. Box 15847 Sacramento, California 95813 Attn: Technical Library 2482-2015A	B. Blubaugh

REPORT COPIES R	D	RECIPIENT	DESIGNEE
1		Aerospace Corporation 2400 E. El Segundo Blvd. Los Angeles, California 90045 Attn: Library-Documents	J. G. Wilder
1		Astropower Laboratory McDonnell-Douglas Aircraft Company 2121 Paularino Newport Beach, California 92163 Attn: Library	
1		DCIC, Battelle Memorial Institute Columbus Lab., Room 11-9012 505 King Avenue Columbus, Ohio 43201 Attn: Library	J. F. Lynch
	1	Battelle Columbus Laboratory	W. H. Safranek
	1	505 King Avenue Columbus, Ohio 43201	R. P. Meister
1		ARO, Incorporated Arnold Engineering Development Center Arnold AF Station, Tennessee 37389 Attn: Library	
1		Bell Aerospace Co. P.O. Box 1 Buffalo, New York 14240 Attn: Library	
1		Boeing Company Space Division P.O. Box 868 Seattle, Washington 98124 Attn: Library	J. D. Alexander C. F. Tiffany
1		Boeing Company P.O. Box 1680 Huntsville, Alabama 35801	Ted Snow
1		Chemical Propulsion Information Agency Applied Physics Laboratory 8621 Georgia Avenue Silver Spring, Maryland 20910	Tom Reedy

REPORT COPIES R	D	RECIPIENT	DESIGNEE
1		Chrysler Corporation Missile Division P.O. Box 2628 Detroit, Michigan Attn: Library	John Gates
1		Chrysler Corporation Space Division P.O. Box 29200 New Orleans, Louisiana 70129 Attn: Librarian	
1		Grumman Aircraft Engineering Corporation Bethpage, Long Island, New York Attn: Library	Joseph Gavin
1		Dunegan/Endevco Rancho Viejo Road San Juan Capistrano, California 92675 Attn: Dr. David Harris	
1		The International Nickel Co. One New York Plaza New York, New York 10004 Attn: Charles B. Sanborn	
1		IIT Research Institute Technology Center Chicago, Illinois 60616 Attn: Library	C. K. Hersh
1		General Dynamics Corp. Convair Aerospace Div. P. O. Box 748 Fort Worth, Texas 76101 Attn: B. O. McCauley	
1		Ling-Temco-Vought Corporation P. O. Box 5907 Dallas, Texas 75222 Attn: Library	
1		Lockheed Missiles & Space Company P.O. Box 504 Sunnyvale, California 94087 Attn: Library	

REPORT COPIES R	D	RECIPIENT	DESIGNEE
1		Lockheed Propulsion Company P.O. Box 111 Redlands, California 92374 Attn: Library, Thackwell	H. L. Thackwell
1		Marquardt Corporation 16555 Saticoy Street Box 2013 - South Annex Van Nuys, California 91409	L. R. Bell, Jr.
1		Denver Division Martin-Marietta Corporation P.O. Box 179 Denver, Colorado 80201 Attn: Library	Dr. Morganthaler F. R. Schwartzberg
1		Lawrence Livermore Laboratory P.O. Box 808 Livermore, California 94550 Attn: Dr. C. A. Tatro	
1		Western Division McDonnell Douglas Astronautics 5301 Bolsa Avenue Huntington Beach, California 92647 Attn: Library	R. W. Hallet G. W. Burge P. Klevatt
1		McDonnell Douglas Aircraft Corporation P.O. Box 516 Lambert Field, Missouri 63166 Attn: Library	R. A. Herzmark
1	1	Rocketdyne Division	D Donald Fulton
	1	North American Rockwell Inc. 6633 Canoga Avenue Canoga Park, California 91304 Attn: Library, Dept. 596-306	Fred Schuler
1		Space & Information Systems Division North American Rockwell 12214 Lakewood Blvd. Downey, California Attn: Library	

REPORT COPIES R	D	RECIPIENT	DESIGNEE
1		Northrop Space Laboratories 3401 West Broadway Hawthorne, California Attn: Library	Dr. Wm. Howard
1		Sandia Laboratories P.O. Box 969 Livermore, California 94550 Attn: J. W. Dini	
1	1	TRW Systems Inc. 1 Space Park Redondo Beach, California 90278 Attn: Tech. Lib. Doc. Acquisitions	Curtis Watts
1	1	TRW TAPCO Division 23555 Euclid Avenue Cleveland, Ohio 44117	Frank Stattler
1		United Aircraft Corporation Corporation Library 400 Main Street East Hartford, Connecticut 06108 Attn: Library	Dr. David Rix Erle Martin Frank Owen Wm. E. Taylor
1		United Aircraft Corporation Pratt & Whitney Division Florida Research & Development Center P.O. Box 2691 West Palm Beach, Florida 33402 Attn: Library	Dr. Schmitke
1		United Aircraft Corporation United Technology Center P.O. Box 358 Sunnyvale, California 94038 Attn: Library	Dr. David Altman
1		University of California Materials Dept. School of Engineering & Applied Science 6531 Boelter Hall Los Angeles, California 90024 Attn: Dr. Kanji Ono	

REPORT COPIES R	D	RECIPIENT	DESIGNEE
1		University of Michigan Dept. of Mechanical Engineering 2046 East Engineering Bldg. Ann Arbor, Michigan 48105 Attn: Dr. J. R. Frederick	
1		Cornell University Lab. of Atomic & Solid State Physics Clark Hall Ithica, New York 14850 Attn: Dr. B. W. Maxfield	